Factors underlying visual illusions are illusion-specific but not feature-specific

Aline F. Cretenoud — Laboratory of Psychophysics, Brain Mind Institute, École Polytechnique Fédérale de Lausanne (EPFL), Lausanne, Switzerland

Harun Karimpur — Experimental Psychology, Justus Liebig University, Giessen, Germany; Center for Mind, Brain and Behavior (CMBB), University of Marburg and Justus Liebig University Giessen, Germany

Lukasz Grzeczkowski — Laboratory of Psychophysics, Brain Mind Institute, École Polytechnique Fédérale de Lausanne (EPFL), Lausanne, Switzerland; General and Experimental Psychology, Psychology Department, Ludwig-Maximilian-University of Munich, Munich, Germany

Gregory Francis — Psychological Sciences, Purdue University, West Lafayette, IN, USA

Kai Hamburger — Experimental Psychology and Cognitive Science, Justus Liebig University, Giessen, Germany

Michael H. Herzog — Laboratory of Psychophysics, Brain Mind Institute, École Polytechnique Fédérale de Lausanne (EPFL), Lausanne, Switzerland

Common factors are ubiquitous. For example, there is a common factor, g, for intelligence. In vision, there is much weaker evidence for such common factors. For example, visual illusion magnitudes correlate only weakly with each other. Here, we investigated whether illusions are hyper-specific as in perceptual learning. First, we tested 19 variants of the Ebbinghaus illusion that differed in color, shape, or texture. Correlations between the illusion magnitudes of the different variants were mostly significant. Second, we reanalyzed a dataset from a previous experiment where 10 illusions were tested under four conditions of luminance and found significant correlations between the different luminance conditions of each illusion. However, there were only very weak correlations between the 10 different illusions. Third, five visual illusions were tested with four orientations. Again, there were significant correlations between the four orientations of each illusion, but not across different illusions. The weak inter-illusion correlations suggest that there is no unique common mechanism for the tested illusions. We suggest that most illusions make up their own factor.

Introduction

Common factors are ubiquitous. For example, it is widely held that there is a common factor, g, for intelligence (Spearman, 1904a). This factor is not measurable per se but is inferred from several indicator

Citation: Cretenoud, A. F., Karimpur, H., Grzeczkowski, L., Francis, G., Hamburger, K., & Herzog, M. H. (2019). Factors underlying visual illusions are illusion-specific but not feature-specific. *Journal of Vision*, *19*(14):12, 1–21, https://doi.org/10.1167/19.14.12.

https://doi.org/10.1167/19.14.12 Received April 24, 2019; published December 12, 2019 ISSN 1534-7362 Copyright 2019 The Authors

variables, such as the Wechsler scale (Wechsler, 2003). In metacognition and somato-sensation, there are common factors between different modalities, for example, between touch and audition (Frenzel et al., 2012). Faivre, Filevich, Solovey, Kühn, and Blanke (2018) showed that participants with high performance in one metacognitive modality are likely to show high performance in other metacognitive modalities.

However, there seems to be no unique common factor explaining individual differences in vision (for a review, see Tulver, 2019). For example, no unique common factor was found for oculomotor tasks (Bargary et al., 2017), bistable paradigms such as binocular rivalry paradigms (Brascamp, Becker, & Hambrick, 2018; Cao, Wang, Sun, Engel, & He, 2018; Wexler, 2005), and face recognition (Verhallen et al., 2017). Rather than a unique common factor, several specific factors underlying individual differences were often suggested. For example, two factors were suggested to underlie the activity of magnocellular and parvocellular systems (Peterzell & Teller, 1996; Simpson & McFadden, 2005; Ward, Rothen, Chang, & Kanai, 2017; but see Goodbourn et al., 2012). Similarly, some very specific factors underlying individual differences have been found in hue scaling (e.g., Emery, Volbrecht, Peterzell, & Webster, 2017a, 2017b) and stereopsis (Peterzell, Serrano-Pedraza, Widdall, & Read, 2017).

Hence, it seems that the structure of individual differences in perception is better represented by a multifactorial space than by a unique common factor. Bosten and colleagues (2017) found that a model with a unique common factor underlying 25 visual and auditory measures only explained about 20% of the total variance. However, eight more specific factors were identified, e.g., a factor related to stereoacuity and one related to oculomotor control, altogether explaining about 57% of the total variance. Additionally, only weak or nonsignificant correlations were found between performance in six very basic visual tasks such as visual backward masking and bisection discrimination (Cappe, Clarke, Mohr, & Herzog, 2014). Aging was expected to strengthen the correlations between visual paradigms because aging effects occur more quickly or strongly for some people. However, only weak correlations were also observed between visual paradigms in older people (Shaqiri et al., 2019).

Interestingly, we also found very weak correlations—except for one—between the magnitudes of visual illusions (Grzeczkowski, Clarke, Francis, Mast, & Herzog, 2017; see also Axelrod, Schwarzkopf, Gilaie-Dotan, & Rees, 2017). Patients with schizophrenia similarly showed only weak correlations between different illusion magnitudes (Grzeczkowski et al., 2018; see also Kaliuzhna et al., 2018).

Improvements in perceptual learning are very specific. For example, when trained with a vertical stimulus, there is usually no transfer of learning to the same stimulus rotated by 90° (e.g., Ball & Sekuler, 1987; Fahle & Morgan, 1996; Grzeczkowski, Cretenoud, Herzog, & Mast, 2017; Schoups, Vogels, & Orban, 1995). Learning was shown to transfer only for stimuli rotated up to 10° as compared to the trained one (Spang, Grimsen, Herzog, & Fahle, 2010). Such a high degree of specificity for the trained orientation suggests that, if perceptual learning plays a role in the perception of illusions, we may even observe only weak correlations between different variants of a given illusion.

Here, we investigated whether factors for illusions are hyper-specific. In Experiment 1, we tested 19 variants of the same illusion, namely the Ebbinghaus illusion, which differed in size, color, shape, or texture. In Experiment 2, the effects of luminance contrast on illusion susceptibility were tested for 10 different visual illusions. In Experiment 3, we measured susceptibility to five visual illusions at different orientations to test whether illusion susceptibility is orientation-specific as in perceptual learning.

Experiment 1

Previously, we observed only weak correlations between the susceptibility to different visual illusions, i.e., a high susceptibility to one illusion does not inevitably imply a high susceptibility to another illusion (Grzeczkowski et al., 2017). Here, we examined to what extent the susceptibility to a single visual illusion (the Ebbinghaus illusion) differs as a function of its size, color, shape, and texture.

Methods

Participants

Participants were 87 visitors of a public event at the École Polytechnique Fédérale de Lausanne (EPFL), Switzerland. Seven of them were considered as outliers and removed from the dataset (see Data analysis section). The age of the remaining 80 participants ranged from 14 to 75 years (mean age: 48 years, 52 females). Adults signed informed consent and parents signed consent for their children. Participation was not compensated for in any form. Procedures were conducted in accordance with the Declaration of Helsinki except for the preregistration (§ 35) and were approved by the local ethics committee.

Apparatus

A BenQ XL2420T monitor (BenQ, Taipei, Taiwan) driven by a PC computer using MATLAB (R2015b, 64 bits; MathWorks, Natick, MA) and the Psychophysics toolbox (Brainard, 1997; Pelli, 1997; version 3.1, 64 bits) was used to present stimuli at a 1920×1080 pixel resolution with a 60 Hz refresh rate and a 32-bit color depth. The distance to the screen was approximately 60 cm. Participants adjusted stimuli with a Logitech LS1 computer mouse. Prior to the experiments the color look-up tables of the monitor were linearized and calibrated with a Minolta LS-100 luminance meter (Konica Minolta, Tokyo, Japan). An experimental room was especially built for this experiment to ensure controlled light conditions.

Stimuli

Each participant was tested on 19 variants of the Ebbinghaus illusion and a control condition (20 conditions in total), shown in Figure 1. For each condition, participants adjusted the size of the right central disk (adjustable target) to match the size of the left central disk (reference target) by moving the mouse on the horizontal axis. The reference target had a fixed diameter of 2.7°. Participants pressed the left mouse button to validate their adjustments. The centers of the left and right central disks were 8.6° to the left and to the right, respectively, and 2.7° to the top and to the bottom compared to the center of the screen.

In a standard variant of the Ebbinghaus illusion (STD), the reference target was a yellow disk surrounded by eight smaller yellow disks (flankers), 1.35° diameter each. The distance between the centers of the reference target and of the small flankers was 2.3°. The right adjustable target was surrounded by 6 large flankers, 3.5° diameter each, which were 4.2° away from the center of the adjustable target. The luminance was approximately 1 cd/m^2 for the background and 146 cd/m^2 for yellow disks.

Bigger and smaller right flankers compared to the STD were shown in the FBIG (right flankers were bigger) and FSMA (right flankers were smaller) conditions. The diameter of the right flankers was 4° and 3°, respectively, and their distance to the center of the adjustable target was 4.7° and 3.6°, respectively.

In the three conditions with either blue flankers, or blue targets, or both (FBLU, TBLU, and BLU), blue-cyan color was used instead of yellow without any further changes compared to the STD condition. Luminance of the blue-cyan color was the same as for the yellow color.

Three conditions used squares instead of disks, either for the flankers (FSQU) or targets (TSQU) or for both flankers and targets (SQU). The sides of the squares were computed so that their surface equals the area of the disks used in the STD condition.

Soccer ball images were shown instead of yellow disks in the FSOC (flankers were soccer balls), TSOC (targets were soccer balls), and SOC (flankers and targets were soccer balls) conditions. Similarly, tennis ball images were used in the FTEN (flankers were tennis balls), TTEN (targets were tennis balls), and TEN (flankers and targets were tennis balls) conditions.

In two conditions, left and right flankers rotated clockwise on a circular orbit with a radius of 2.3° and 4.2°, respectively. The motion speed was either "slow" with 0.5 radian per refreshing screen (SRT for slow rotation) or "fast" with 1 radian per refreshing screen (FRT for fast rotation).

In the MRF (missing right flankers) conditions, the right flankers were removed. Likewise, the left flankers were missing in the MLF (missing left flankers) condition. Finally, we used a control condition without flankers (CON).

Procedure

The experimenter first explained the task to the participants who completed one trial of the standard variant of the illusion (STD) to familiarize themselves with the adjustment method. Then, each condition was presented twice. The two trials for each condition were presented sequentially, i.e., one after the other, and without time constraint. The order of the 20 conditions was randomized across participants. The initial size of the adjustable target was pseudorandomly chosen for each trial. The adjustable target appeared with a diameter in the range of 0° to 4.5° in the case of a circular target, except for the FBIG and FSMA conditions where the ranges were 0° to 4.9° and 0° to 3.8°, respectively. When the adjustable target was a square, the initial side of the square was pseudorandomly chosen between 0° and 3.99°, to match the global target area observed in case of a circular target.

The experimenter stayed in the experimental room during the whole experiment to answer any questions. Participants were asked to base their adjustments on their subjective perception only and to ignore potential prior knowledge about the illusion. At the end, participants were shown their results for the nine following conditions: STD, FBIG, TBLU, BLU, TSQU, SQU, SOC, TEN, and SRT.

Data analysis

As a measure of illusion magnitude for each participant and each condition, the adjusted radii (or side lengths, in case of a square target) from both trials were averaged into a mean adjustment, from which the reference disk radius (or reference side length) was

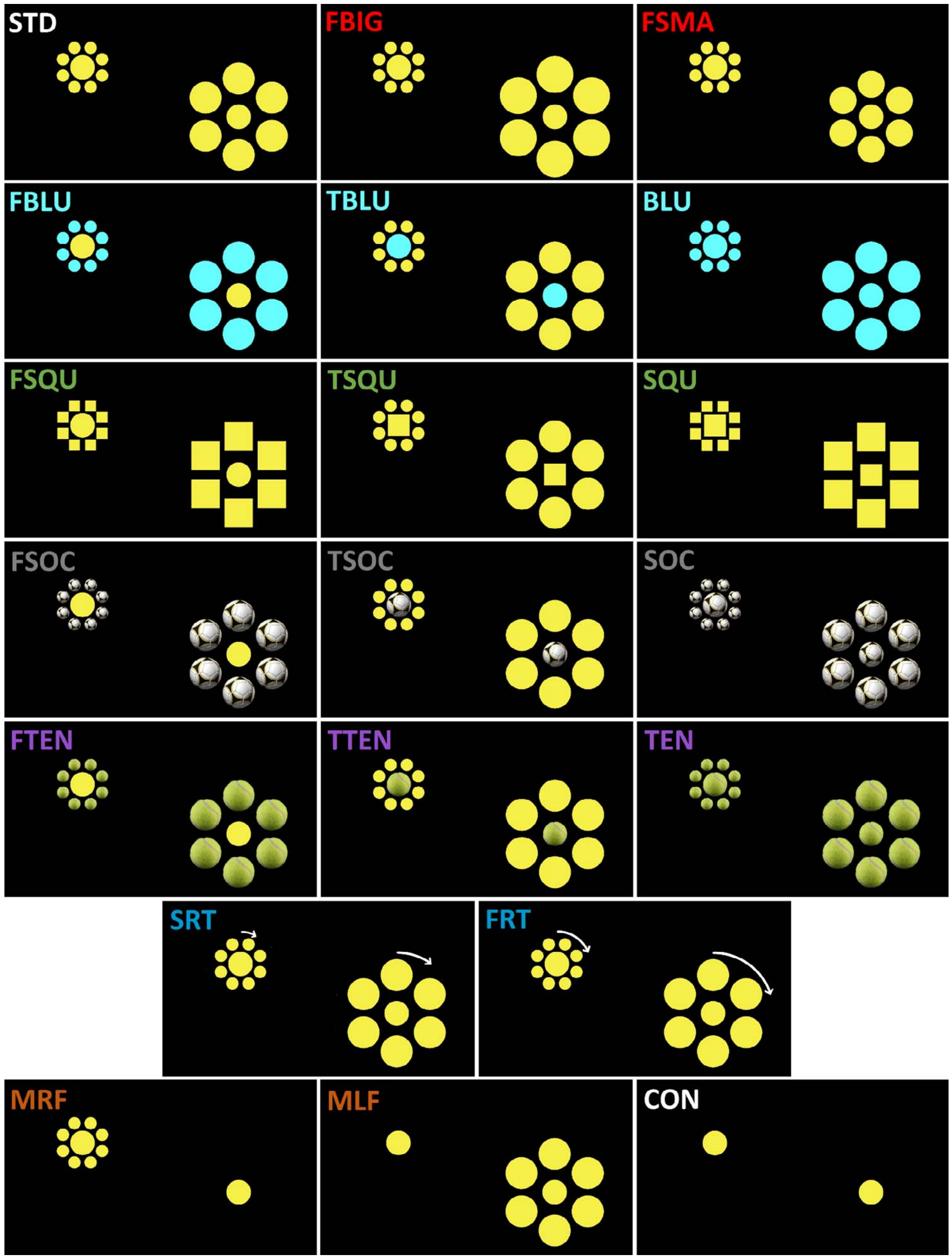

Figure 1. In 19 variants of the Ebbinghaus illusion and a control condition, participants adjusted the size of the right central disk (adjustable target) to match the size of the left central disk (reference target) by moving the mouse on the horizontal axis. The conditions of the illusion varied from the standard one (STD) as follows: bigger right flankers (FBIG), smaller right flankers (FSMA), blue flankers (FBLU), blue targets (TBLU), both blue flankers and targets (BLU), square flankers (FSQU), square targets (TSQU), both square flankers and targets (SQU), soccer ball flankers (FSOC), soccer ball targets (TSOC), both soccer ball flankers and targets (SOC), tennis ball flankers (FTEN), tennis ball targets (TTEN), both tennis ball flankers and targets (TEN), slow clockwise rotation of the flankers (SRT), fast clockwise rotation of the flankers (FRT), missing right flankers (MRF), missing left flankers (MLF), and missing all flankers (CON). For each condition, participants performed two adjustment trials. The different conditions were presented in a random order for each participant. The acronyms of similar conditions are presented in the same color.

subtracted. The result was divided by the reference disk radius (or reference side length) to express the illusion magnitude proportionally to the reference disk radius (or reference side length). A positive illusion magnitude indicates that the adjustable target looked smaller than the reference target and thereby needed to be over-adjusted in order to appear the same size. A negative illusion magnitude indicates that the adjustable target looked larger than the reference target and thereby needed to be underadjusted in order to appear the same size. Analyses were performed with MATLAB (R2015b, 64 bit) and R (R Development Core Team, 2018).

Shapiro–Wilk tests, which test the null hypothesis that a sample comes from a normally distributed population, indicated that all distributions were approximately normally distributed. Data were therefore not transformed for further analyses.

Since data are roughly normally distributed and to ensure maximal power, we computed parametric tests with outlier removal rather than nonparametric statistics. For outlier detection, we used a modified z-score, which is more robust than the commonly used z-score (Iglewicz & Hoaglin, 1993). The modified z-score takes into account the median ($\tilde{x}$) and median absolute deviation (MAD) of a given condition instead of the mean and standard deviation, respectively, and is computed as:

$$M_i = \frac{0.6745(x_i - \tilde{x})}{\mathrm{MAD}}$$

As suggested by Iglewicz and Hoaglin (1993), modified z-scores with an absolute value greater than 3.5 were considered as outliers. Seven participants showed at least one condition with a modified z-score larger than ± 3.5 and were removed from the dataset.

Following Shrout and Fleiss (1979) and Koo and Li (2016), intrarater reliability was assessed by computing two-way mixed effects models (intraclass correlations of type (3, 1) or $ICC_{3,1}$) between the two adjustments of each condition. Bravais–Pearson's correlations were computed between the mean magnitude of each condition and participants' age.

The mean illusion magnitude of the control condition was significantly different from zero (see the Magnitudes of the illusions section), which indicates a bias that probably occurred in all conditions. Therefore, we computed Bravais–Pearson's partial correlations to examine the relationships between the mean magnitudes for each pair of variants, controlling for the control condition variability. A cutoff value of 0.3 for the correlation coefficient (r) reflects the lower limit for a medium effect size according to Cohen (1988), and a relatively large effect size according to Hemphill (2003; see also Gignac & Szodorai, 2016). The observed between-variant partial correlations were underestimated because of measurement errors (Spearman, 1904b; Wang, 2010), which are reflected by moderate intrarater reliabilities (see the Intrarater reliability section). To account for these measurement errors, which put an upper limit on the between-variant correlations, we also computed disattenuated partial correlations (Osborne, 2003):

$$r_{xy,z'} = \frac{r_{zz}r_{xy} - r_{xz}r_{yz}}{\sqrt{r_{xx}r_{zz} - r_{xz}^2}\sqrt{r_{yy}r_{zz} - r_{yz}^2}}$$

where $r_{xy,z'}$ is the disattenuated relationship between x and y controlling for the z variable; r_{xx}, r_{yy}, and r_{zz} are the intrarater reliabilities of the x, y, and z variables and r_{xy}, r_{xz}, and r_{yz} are the attenuated (i.e., non-disattenuated) correlation coefficients between the pairs of variables.

An exploratory factor analysis (EFA) was computed to explore the factors underlying the global structure of the Ebbinghaus illusion using the guidelines outlined in Preacher, Zhang, Kim, and Mels (2013).

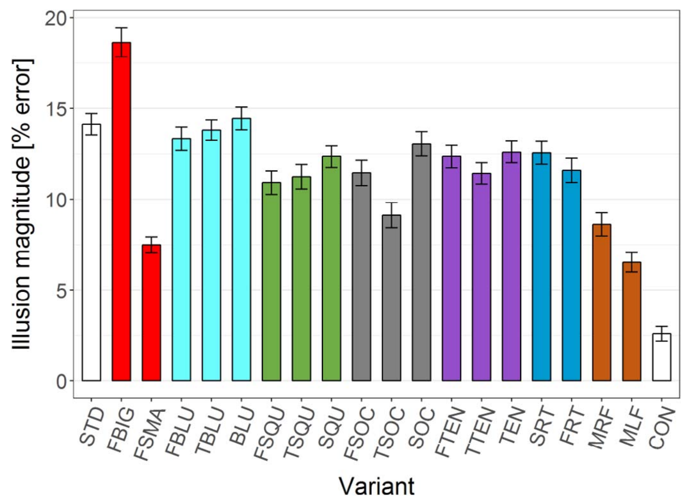

Figure 2. Illusion magnitudes [% error] $\pm$ *SEM* for the 19 variants of the Ebbinghaus illusion and a control condition. Similar conditions are presented in the same color, as in Figure 1.

Results

Magnitudes of the illusions

Participants significantly overadjusted the right target compared to the left reference (Figure 2) in all 20 conditions (independent one-sample t test for each condition: $p < 0.001$), including the control condition (CON, illusion magnitude: $2.595\% \pm 0.399\%$, $t[79] = 6.508$, $p < 0.001$, Cohen's $d = 0.728$).

Intrarater reliability

Moderate but significant intraclass correlations were observed for all 20 conditions even after correcting for inflated family-wise errors (Table 1, diagonal).

Correlations between illusion magnitudes and age

Contrary to previous findings (Grzeczkowski et al., 2017), none of the conditions correlated significantly with age after Bonferroni correction was applied for multiple comparisons.

Partial correlations between illusion magnitudes

To control for the CON condition variability, which showed up as a significant effect in the CON condition,

	STD	FBIG	FSMA	FBLU	TBLU	BLU	FSQU	TSQU	SQU	FSOC	TSOC	SOC	FTEN	TTEN	TEN	SRT	FRT	MRF	MLF
STD	.59	.59	.52	.39	.56	.40	.41	.38	.39	.29	.34	.50	.43	.48	.29	.48	.44	.30	.23
FBIG	.93	.72	.50	.60	.63	.49	.50	.33	.59	.45	.37	.57	.55	.35	.43	.63	.56	.33	.36
FSMA	.96	.84	.50	.46	.54	.30	.34	.38	.57	.36	.42	.62	.52	.30	.49	.52	.49	.27	.38
FBLU	.65	.86	.81	.67	.63	.60	.36	.28	.45	.52	.39	.45	.58	.35	.30	.45	.48	.30	.34
TBLU	.98	.97	1	1	.60	.52	.53	.44	.53	.50	.52	.61	.59	.47	.43	.55	.55	.29	.35
BLU	.67	.73	.53	.95	.86	.63	.42	.30	.40	.49	.38	.41	.46	.43	.36	.47	.47	.24	.30
FSQU	1	1	.84	.71	1	.91	.44	.46	.39	.43	.42	.43	.51	.61	.41	.49	.47	.21	.14
TSQU	.72	.48	.74	.39	.76	.48	1	.59	.46	.36	.32	.46	.39	.45	.31	.33	.27	.25	.29
SQU	.74	1	1	.79	1	.72	.95	.89	.50	.45	.46	.65	.55	.41	.58	.51	.39	.40	.41
FSOC	.46	.63	.61	.77	.79	.75	.90	.56	.77	.68	.47	.40	.54	.29	.40	.58	.49	.18	.30
TSOC	.57	.51	.74	.56	.84	.57	.87	.48	.81	.71	.65	.58	.58	.47	.45	.48	.46	.37	.22
SOC	.89	.89	1	.70	1	.66	.95	.79	1	.63	.95	.60	.57	.50	.54	.54	.50	.33	.25
FTEN	.79	.86	1	.94	1	.76	1	.63	1	.87	.97	.99	.60	.51	.53	.55	.53	.27	.31
TTEN	.86	.52	.55	.54	.81	.71	1	.78	.76	.43	.77	.87	.90	.58	.49	.40	.49	.31	.16
TEN	.61	.69	1	.44	.78	.63	.85	.44	1	.68	.76	1	.97	.93	.60	.53	.42	.23	.40
SRT	.82	.96	.97	.69	.93	.76	1	.53	.94	.91	.76	.92	.96	.66	1	.61	.76	.10	.37
FRT	.76	.83	.88	.72	.90	.74	1	.37	.68	.75	.69	.81	.87	.82	.70	1	.65	.15	.24
MRF	.56	.49	.51	.44	.46	.37	.32	.35	.76	.24	.59	.54	.40	.51	.26	.10	.15	.57	.16
MLF	.38	.52	.69	.51	.55	.47	.23	.46	.73	.44	.31	.39	.49	.22	.71	.59	.35	.22	.63

Table 1. Diagonal (in gray): Intrarater reliability expressed as intraclass correlation coefficients ($ICC_{3,1}$) for each variant. All of them were significant. Upper triangle: Attenuated partial correlation coefficients between each pair of variants (Bravais–Pearson's *r*), controlling for the control condition variability. Lower triangle: Disattenuated partial correlation coefficients between each pair of variants (Bravais-Pearson's *r*), controlling for the control condition variability. Italics and bold font indicate significant results without and with Bonferroni correction, respectively. The color scale from white to red reflects effect sizes from $r = 0$ to $r = 1$. The acronyms of similar variants are presented in the same color, as in Figure 1.

partial correlations were computed for each pair of variants based on the mean of both adjustments for each participant. We analyzed attenuated (Table 1, upper triangle) and disattenuated (Table 1, lower triangle) partial correlation coefficients without and with Bonferroni correction and observed strong between-variant effects. Indeed, out of 171 attenuated correlations only 26 showed $r < 0.3$. Similarly, only seven disattenuated correlations showed $r < 0.3$ (Figure 3).

Exploratory factor analysis (EFA)

A one-factor model (explaining ~44% of the variance) was suggested by a parallel analysis and scree plot inspection. All conditions except the CON condition highly loaded onto a unique factor (factor loadings—STD: 0.600; FBIG: 0.764; FSMA: 0.671; FBLU: 0.692; TBLU: 0.799; BLU: 0.642; FSQU: 0.676; TSQU: 0.580; SQU: 0.729; FSOC: 0.647; TSOC: 0.670; SOC: 0.778; FTEN: 0.787; TTEN: 0.647; TEN: 0.684; SRT: 0.757; FRT: 0.722; MRF: 0.436; MLF: 0.451; CON: 0.293).

Data simulation

As an estimate of the experimental power, we simulated data to estimate the likelihood to observe at least 145 out of 171 correlations with $r > 0.3$ if there truly are no correlations between the variants. Individual mean adjustments for all 19 variants were simulated from a normal distribution ($M = 0$, $SD = 1$) and correlation coefficients were computed from these simulated values. The probability of observing at least 145 correlations with $r > 0.3$ averaged across 10,000 simulations was smaller than 0.001. Similarly, this probability was also smaller than 0.001 when we simulated weak correlation coefficients from a normal distribution with mean and standard deviation computed from the inter-illusion

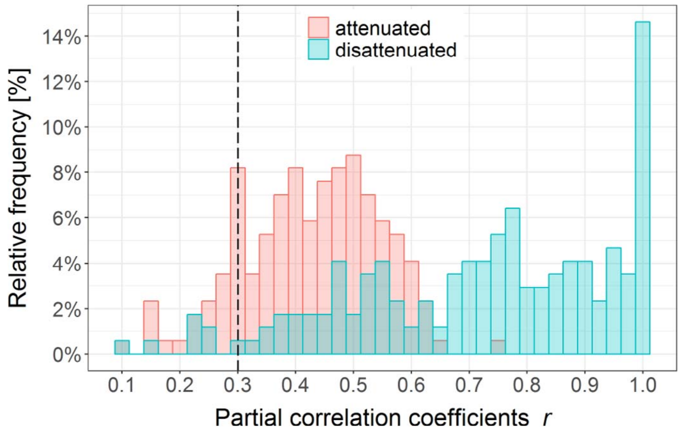

Figure 3. Relative frequency (in percentage) of attenuated (red) and disattenuated (turquoise) partial correlation coefficients r in Experiment 1. According to Cohen's convention (Cohen, 1988), $r = 0.3$ (vertical dashed line) is the lower limit corresponding to a medium effect size. Only 26 attenuated and seven disattenuated correlation coefficients out of 171 showed $r < 0.3$.

correlation coefficients of Experiment 3 ($M = 0.16$, $SD = 0.12$; see Experiment 3 Relations between illusion magnitudes section), suggesting that our results are unlikely to be false alarms. However, when simulating r coefficients from a normal distribution centered on the average attenuated correlation coefficient, the likelihood of observing at least 145 out of 171 correlations with $r > 0.3$ was 0.74, which suggests that a new study with our sample size has a pretty good chance of showing a similar pattern of results.

Experiment 2

Hamburger, Hansen, and Gegenfurtner (2007) previously tested 10 visual illusions under different luminance conditions and observed high correlations between the different luminance conditions for each illusion. However, the authors did not analyze the relationships between the different illusions, which we did here. We added four subjects who joined a pilot experiment in 2007. There are no changes between the pilot and the reported experiment.

Methods

Participants

Twenty-one students (nine females, mean age: 26 years, age range: 20–48 years) of the Justus Liebig University Giessen (JLU), Germany, were considered for the analysis (three outliers; see Data analysis section). Participants signed informed consent and received course credits for participation. Participants had to correctly answer all Ishihara pseudo-isochromatic plates to take part in this experiment. Procedures were conducted in accordance with the Declaration of Helsinki except for the preregistration (§ 35) and were approved by the local ethics committee.

Apparatus

The experiment was conducted in a dark room. The distance between the participant and the monitor was 60 cm and a chinrest was used for head stabilization, but participants were free to move their eyes. Observation was binocular and the stimuli were presented in the center of the monitor at the line of sight. The stimuli were presented on a 21-in. Iiyama Vision Master Pro 513 CRT monitor at a refresh rate of 85 Hz noninterlaced with a resolution of 1154 × 768 pixels, driven by an NVIDIA graphics card with a color resolution of 8 bits for each of the three monitor primaries. We linearized the relationship between luminance and voltage output by a color look-up table for each primary.

Color space

Four different luminance/color conditions were included (Figure 4): a high luminance contrast condition (50%; Lum), a low luminance contrast condition (10%; LumLow), a "red-green" [L – M] isoluminant condition (Iso), and a "blue-yellow" [S – (L + M)] isoluminant condition (IsoS). Both isoluminant conditions were derived from the DKL color space (Derrington, Krauskopf, & Lennie, 1984; Krauskopf, Williams, & Heeley, 1982).

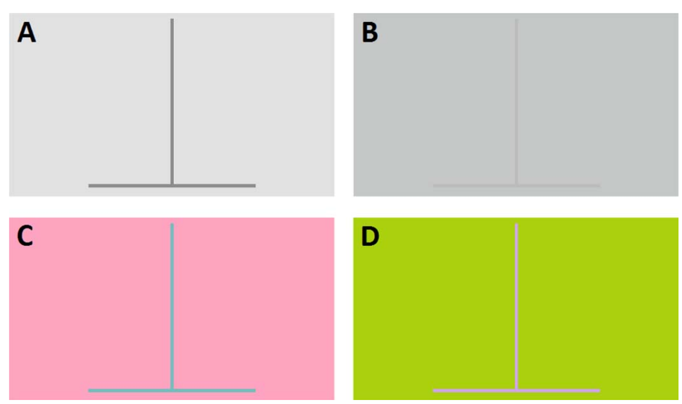

Figure 4. Exemplary horizontal-vertical stimulus with two luminance conditions: (A) 50% (Lum) and (B) 10% (LumLow) contrast and two isoluminant color conditions: (C) L – M (Iso) and (D) S – (L + M) (IsoS) according to DKL color space (Derrington et al., 1984). Please note that the colors here may vary in luminance due to reproduction.

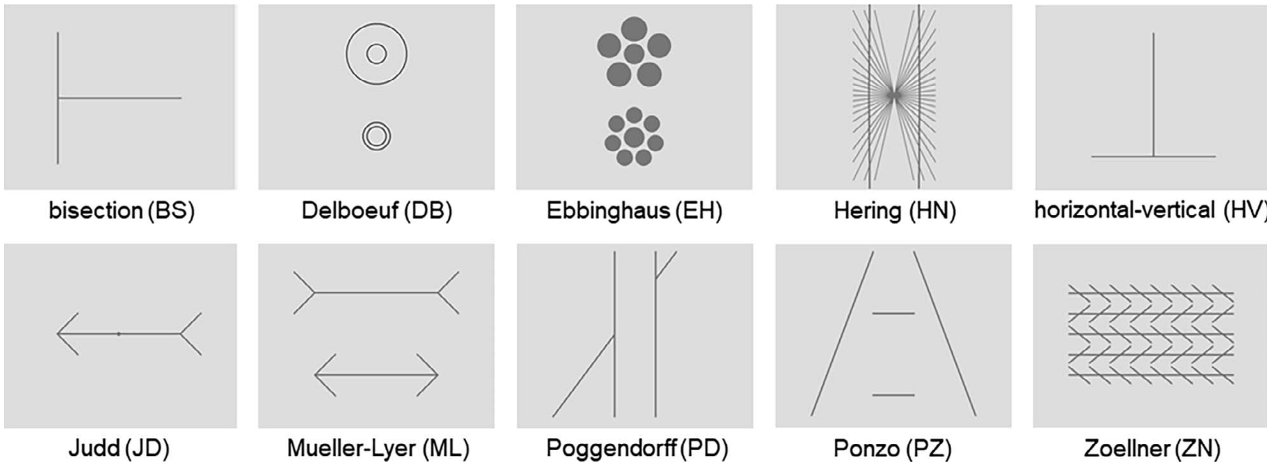

Figure 5. The 10 visual illusions used in Experiment 2. Observers were asked to reach subjective equality in length (BS, HV, JD, ML, PZ), size (DB, EH), curvature (HN), position (PD), and orientation (ZN) with an adjustment procedure. For a detailed description of the different adjustments, please see Hamburger et al. (2007).

Stimuli

The stimuli consisted of 10 classic visual illusions (Figure 5). These illusions were: bisection (BS), Delboeuf (DB), Ebbinghaus (EH), Hering (HN), horizontal-vertical (HV), Judd (JD), Müller-Lyer (ML), Poggendorff (PD), Ponzo (PZ), and Zöllner (ZN). Stimuli were created with the Psychophysics Toolbox (Brainard, 1997; Pelli, 1997) in MATLAB (version 7, 32 bit). Stimulus size (including the background) was 17° of the visual field for all illusions with a constant line width of 4 pixels (0.14°). Only in the HN illusion the radial lines have a smaller width of 1 pixel (0.035°) in order to retain clearly visible edges within the illusion.

Procedure

The instruction for the participants was to reach subjective equality in length (BS, HV, JD, ML, PZ), size (DB, EH), curvature (HN), position (PD), and orientation (ZN) by pressing the right and left arrow keys of a standard keyboard. The stimulus conditions were randomly intermixed and each illusion was presented under four different luminance conditions, four trials each (160 trials in total). For a detailed description of the methods please see Hamburger et al. (2007).

Data analysis

We first aggregated the 10 illusion magnitudes for each of the four luminance conditions and all participants over all trials. We then standardized these results for each illusion by computing modified z-scores as in Experiment 1 to allow comparison across the different illusions. Three participants showed modified z-scores larger than ± 3.5 in at least one condition and were removed from the dataset. A repeated-measures analysis of variance (ANOVA) with two main factors (illusion and luminance condition) was computed. As in Experiment 1, we computed intrarater reliability between the four adjustments of each condition. We computed Bravais–Pearson's r correlation coefficients between illusion magnitudes over all illusions and luminance conditions and computed disattenuated correlation coefficients as:

$$r_{xy'} = \frac{r_{xy}}{\sqrt{r_{xx} r_{yy}}}$$

where $r_{xy'}$ is the disattenuated relationship between x and y, r_{xx} and r_{yy} are the intrarater reliabilities of the x and y variables, and r_{xy} is the attenuated correlation coefficient between x and y. Similarly to Experiment 1, we conducted an EFA. Oblique rotations allow factors to correlate, while uncorrelated factors result from orthogonal rotations. Since we have no reason to preclude correlated factors from our datasets, we used an oblique rotation (promax) for the maximum likelihood estimation rather than an orthogonal rotation. If the factors are uncorrelated, both oblique and orthogonal rotations produce very similar results (e.g., Costello & Osborne, 2005).

Results

Magnitudes of the illusions

Figure 6 shows the standardized illusion magnitudes as a function of illusion and luminance conditions. The z-scores show to what extent the illusion magnitudes deviate as a function of luminance for each illusion type (see Hamburger et al., 2007, for the nontransformed illusion magnitudes). A repeated-measures ANOVA with illusion and luminance conditions as within-subject factors yielded no significant main effect of

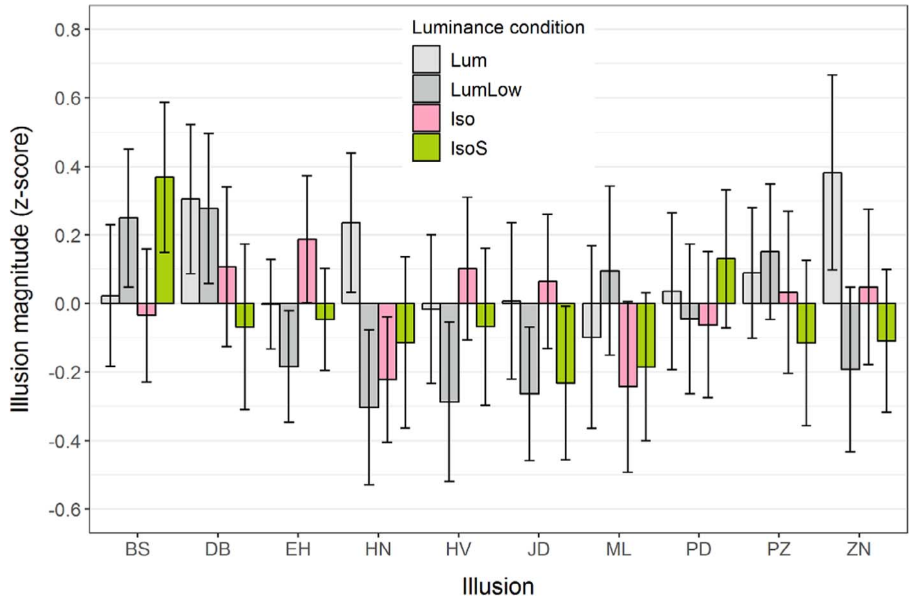

Figure 6. Standardized illusion magnitudes ± *SEM* as a function of illusion and luminance conditions. The *z*-scores show to what extent the illusion magnitudes deviate as a function of luminance for each illusion type.

illusion ($p = 0.980$) but a significant main effect of luminance condition ($F[3, 60] = 4.292$, $p = 0.008$, $\eta_p^2 = 0.177$) and a significant interaction between illusion and luminance condition ($F[27, 540] = 3.679$, $p < 0.001$, $\eta_p^2 = 0.155$).

Intrarater reliability

For each combination of illusion and luminance condition, we computed intraclass correlations ($ICC_{3,1}$) between the adjustments of all participants (Table 2, diagonal). For all but three conditions we found significant intraclass correlations after correcting the alpha level for inflated family-wise errors. In those three cases, the intraclass correlations yielded significance without correction (EH-IsoS: ICC coef. = 0.225, 95% CI [0.027, 0.488], $F[20, 60] = 2.164$, $p = 0.011$; ZN-Iso: ICC coef. = 0.218, 95% CI [0.022, 0.481], $F[20, 60] = 2.117$, $p = 0.013$; ZN-IsoS: ICC coef. = 0.228, 95% CI [0.030, 0.491], $F[20, 60] = 2.182$, $p = 0.011$).

Correlations between illusion magnitudes

We show both attenuated (Table 2, upper triangle) and disattenuated (Table 2, lower triangle) correlation coefficients without and with Bonferroni correction. Among 780 correlations, 253 attenuated and 455 disattenuated correlations resulted in $r > 0.3$. For each illusion, the different luminance conditions were highly correlated ($r > 0.3$ for all intra-illusion correlations), while 27% (193 out of 720) and 55% (395 out of 720) of the attenuated and disattenuated inter-illusion correlations showed $r > 0.3$, respectively (Figure 7). More specifically, it seems that most illusions were not strongly related to each other, except the BS illusion, which was strongly linked to the HV illusion. In fact, the BS illusion is an HV illusion rotated by 90°.

Exploratory factor analysis (EFA)

We inspected the scree plot of the EFA and identified nine factors. These factors accounted for ~90% of the variance (RF1: 18%, RF2: 11%, RF5: 10%, RF3: 10%, RF4: 9%; RF6: 8%; RF8: 8%; RF7:

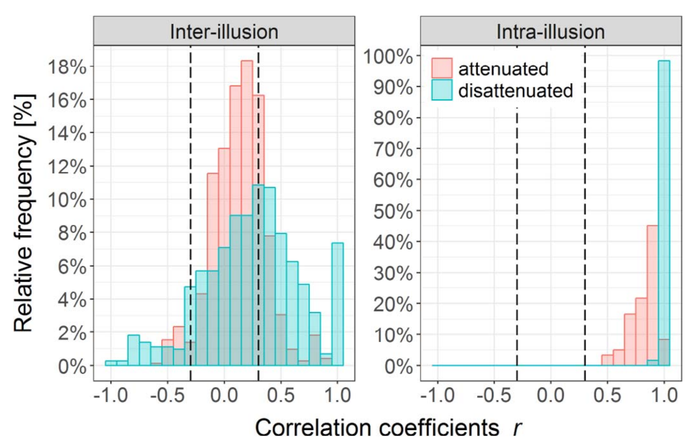

Figure 7. Relative frequency (in percentage) of attenuated (red) and disattenuated (turquoise) correlation coefficients *r* for inter- (left panel) and intra-illusion (right panel) correlations in Experiment 2. According to Cohen's convention (Cohen, 1988), $r = \pm 0.3$ (vertical dashed lines) is the lower limit corresponding to a medium effect size. Please note the different scales of the *y* axes.

	BS Lum	BS LumLow	BS Iso	BS IsoS	DB Lum	DB LumLow	DB Iso	DB IsoS	EH Lum	EH LumLow	EH Iso	EH IsoS	HN Lum	HN LumLow	HN Iso	HN IsoS	HV Lum	HV LumLow	HV Iso	HV IsoS	JD Lum	JD LumLow	JD Iso	JD IsoS
BS Lum	.67	.90	.92	.87	.00	.02	-.08	-.06	.10	.03	.09	-.02	.01	.01	-.24	.16	.80	.78	.79	.77	.39	.13	.27	.30
BS LumLow	1	.42	.91	.96	.25	.29	.19	.16	.06	.00	.04	.07	.20	.11	-.07	.32	.81	.82	.85	.84	.27	-.02	.33	.34
BS Iso	1	1	.70	.92	.06	.14	.06	.05	.14	.04	.16	.13	.08	.10	-.08	.28	.88	.87	.88	.84	.41	.20	.44	.41
BS IsoS	1	1	1	.55	.09	.13	.03	.00	.04	-.01	.06	.03	.13	.04	-.13	.25	.81	.80	.82	.82	.36	.07	.36	.37
DB Lum	.00	.48	.09	.15	.67	.96	.93	.89	-.21	-.33	-.08	.20	.15	.16	.16	.34	.07	.04	.19	.13	-.48	-.43	.04	-.10
DB LumLow	.02	.53	.19	.21	1	.71	.98	.93	-.10	-.19	.01	.28	.23	.20	.21	.40	.13	.11	.22	.15	-.43	-.40	.17	-.10
DB Iso	-.10	.34	.08	.04	1	1	.79	.97	-.05	-.15	.02	.32	.25	.24	.27	.41	.07	.05	.16	.10	-.49	-.42	.11	-.14
DB IsoS	-.08	.27	.07	.00	1	1	1	.79	.04	-.11	.09	.33	.18	.20	.13	.35	.09	.02	.11	.06	-.43	-.37	.12	-.15
EH Lum	.20	.14	.27	.10	-.43	-.19	-.10	.07	.37	.89	.74	.74	.24	.14	-.02	-.10	.26	.25	.10	.24	.48	.46	.52	.31
EH LumLow	.05	.00	.07	-.01	-.52	-.29	-.22	-.16	1	.61	.60	.64	.33	.21	.11	-.05	.14	.22	.04	.19	.36	.33	.35	.19
EH Iso	.13	.07	.24	.10	-.12	.02	.03	.12	1	.94	.68	.78	.35	.30	.16	-.05	.30	.30	.19	.19	.35	.35	.53	.21
EH IsoS	-.05	.24	.33	.09	.51	.70	.75	.79	1	1	1	.23	.44	.37	.37	.13	.28	.33	.27	.32	.09	.17	.48	.12
HN Lum	.01	.46	.14	.26	.26	.39	.41	.29	.57	.60	.61	1	.48	.83	.75	.72	.13	.24	.24	.26	-.01	-.11	.25	.13
HN LumLow	.02	.25	.18	.08	.28	.35	.40	.33	.33	.38	.54	1	1	.47	.77	.82	.24	.29	.31	.28	.10	.02	.24	.24
HN Iso	-.50	-.18	-.15	-.30	.32	.42	.50	.25	-.05	.23	.32	1	1	1	.36	.65	-.04	.14	.19	.10	-.20	-.11	.11	.07
HN IsoS	.24	.63	.42	.42	.52	.60	.58	.50	-.21	-.09	-.08	.34	1	1	1	.64	.28	.29	.36	.35	-.01	-.13	.22	.15
HV Lum	1	1	1	1	.10	.18	.09	.12	.51	.21	.43	.70	.23	.41	-.08	.42	.72	.92	.92	.90	.45	.19	.42	.40
HV LumLow	1	1	1	1	.06	.16	.07	.03	.49	.34	.44	.83	.41	.51	.29	.43	1	.69	.95	.91	.32	.09	.29	.32
HV Iso	1	1	1	1	.32	.35	.24	.17	.22	.07	.31	.78	.46	.62	.43	.61	1	1	.55	.93	.25	.04	.32	.37
HV IsoS	1	1	1	1	.19	.20	.13	.08	.45	.28	.26	.79	.43	.48	.19	.51	1	1	1	.75	.30	.09	.29	.38
JD Lum	.68	.61	.71	.70	-.85	-.73	-.79	-.70	1	.67	.61	.28	-.01	.20	-.49	-.01	.76	.55	.48	.50	.48	.81	.70	.78
JD LumLow	.26	-.05	.38	.14	-.84	-.75	-.75	-.67	1	.67	.68	.58	-.26	.04	-.30	-.25	.35	.16	.09	.16	1	.39	.68	.75
JD Iso	.53	.80	.83	.76	.08	.31	.20	.22	1	.70	1	1	.58	.54	.28	.45	.78	.56	.68	.52	1	1	.40	.72
JD IsoS	.56	.79	.75	.76	-.19	-.17	-.24	-.26	.79	.37	.39	.39	.30	.54	.17	.28	.71	.59	.75	.66	1	1	1	.44
ML Lum	.06	.40	.41	.36	.29	.49	.47	.43	-.22	-.11	.04	.06	.27	.23	.15	.47	.27	.25	.18	.18	-.11	-.02	.32	.02
ML LumLow	.12	.47	.44	.37	.43	.59	.55	.43	-.57	-.27	-.04	.00	.31	.38	.39	.55	.36	.38	.39	.29	-.32	-.34	.13	-.17
ML Iso	.15	.37	.43	.36	.11	.30	.28	.21	-.45	-.19	-.08	-.31	.27	.42	.30	.63	.33	.26	.27	.21	.06	.07	.35	.11
ML IsoS	.04	.29	.42	.28	.15	.35	.35	.27	-.23	.02	-.02	.13	.43	.70	.63	.80	.32	.32	.32	.27	.13	.38	.55	.34
PD Lum	.75	.84	.75	.57	.06	.07	.08	.03	.41	.20	.30	.09	.42	.29	.04	.27	.53	.53	.60	.65	.51	.65	.58	.96
PD LumLow	.58	.69	.55	.53	-.16	-.14	-.12	-.17	.58	.33	.44	.27	.77	.28	.16	.22	.27	.30	.31	.48	.48	.70	.61	.86
PD Iso	.51	.61	.52	.51	-.11	-.13	-.14	-.22	.04	-.01	.30	-.06	.75	.52	.43	.38	.33	.39	.47	.50	.32	.45	.35	.78
PD IsoS	.57	.70	.61	.53	-.02	-.06	.01	-.10	-.04	-.09	.10	-.12	.69	.46	.43	.46	.42	.45	.59	.68	.05	.33	.10	.59
PZ Lum	-.34	-.26	-.26	-.21	.21	.18	.09	-.03	-.63	-.25	-.04	-.27	.22	.21	.16	-.10	-.25	.01	-.09	-.21	-.52	-.84	-.65	-.34
PZ LumLow	-.75	-1	-.70	-.85	-.25	-.27	-.27	-.23	-.03	.10	.17	-.24	-.42	-.26	-.15	-.62	-.82	-.59	-.80	-.80	-.26	-.02	-.47	-.12
PZ Iso	-.81	-1	-.78	-.94	-.11	-.13	-.10	-.04	-.20	.02	.25	-.30	-.03	.36	.32	-.18	-.77	-.65	-.76	-.82	-.22	.00	-.29	.04
PZ IsoS	-.58	-.80	-.48	-.56	-.12	-.05	-.09	-.10	.06	.13	.40	.10	-.01	-.03	.20	-.31	-.62	-.44	-.59	-.65	-.08	.04	.11	.02
ZN Lum	.18	.53	.42	.37	.16	.42	.38	.28	1	1	.74	1	.96	.73	.72	.48	.56	.66	.59	.59	.47	.45	1	.49
ZN LumLow	.11	.45	.54	.37	.36	.65	.66	.64	1	.98	.94	1	.84	.69	.67	.54	.63	.66	.61	.64	.24	.43	1	.46
ZN Iso	-.18	.40	.16	.29	.77	1	.99	.92	1	1	1	1	1	1	1	.78	.46	.55	.53	.54	-.19	-.18	1	-.17
ZN IsoS	-.32	.30	.08	.10	1	1	1	1	1	.61	1	1	1	.89	.94	.75	.24	.18	.20	.17	-.06	-.11	1	.26

	ML Lum	ML LumLow	ML Iso	ML IsoS	PD Lum	PD LumLow	PD Iso	PD IsoS	PZ Lum	PZ LumLow	PZ Iso	PZ IsoS	ZN Lum	ZN LumLow	ZN Iso	ZN IsoS
BS Lum	.05	.08	.11	.03	.44	.32	.32	.32	-.19	-.41	-.47	-.39	.11	.06	-.07	-.13
BS LumLow	.22	.24	.21	.15	.39	.31	.30	.31	-.11	-.50	-.56	-.42	.26	.20	.12	.09
BS Iso	.29	.30	.31	.28	.46	.32	.33	.35	-.14	-.39	-.46	-.32	.26	.31	.06	.03
BS IsoS	.23	.22	.24	.17	.31	.27	.29	.27	-.10	-.43	-.50	-.34	.21	.19	.10	.03
DB Lum	.21	.28	.08	.10	.03	-.09	-.07	-.01	.11	-.14	-.06	-.08	.10	.20	.29	.46
DB LumLow	.35	.40	.22	.24	.05	-.08	-.09	-.03	.10	-.15	-.08	-.04	.27	.38	.43	.57
DB Iso	.36	.39	.22	.25	.05	-.08	-.10	.01	.06	-.16	-.06	-.07	.25	.40	.41	.58
DB IsoS	.33	.31	.16	.19	.02	-.10	-.15	-.06	-.02	-.14	-.03	-.07	.18	.39	.38	.56
EH Lum	-.12	-.28	-.24	-.11	.18	.24	.02	-.02	-.26	-.01	-.08	.03	.57	.56	.45	.37
EH LumLow	-.07	-.17	-.13	.02	.11	.18	-.01	-.05	-.13	.05	.01	.08	.62	.53	.47	.23
EH Iso	.03	-.02	-.06	-.01	.18	.25	.19	.06	-.02	.09	.15	.27	.46	.53	.45	.44
EH IsoS	.02	.00	-.13	.05	.03	.09	-.02	-.04	-.09	-.08	-.10	.04	.63	.69	.70	.54
HN Lum	.16	.17	.16	.24	.21	.37	.40	.33	.10	-.19	-.02	-.01	.50	.40	.50	.45
HN LumLow	.14	.21	.25	.39	.14	.13	.27	.22	.10	-.12	.18	-.02	.38	.33	.33	.29
HN Iso	.08	.19	.16	.31	.02	.07	.20	.18	.07	-.06	.14	.10	.33	.28	.35	.27
HN IsoS	.32	.36	.44	.51	.16	.12	.23	.25	-.05	-.33	-.10	-.20	.29	.30	.29	.29
HV Lum	.20	.25	.24	.22	.33	.16	.22	.24	-.14	-.47	-.47	-.43	.36	.37	.18	.10
HV LumLow	.18	.26	.19	.21	.32	.17	.25	.26	.01	-.33	-.38	-.30	.41	.38	.21	.07
HV Iso	.11	.23	.18	.19	.32	.16	.27	.30	-.05	-.40	-.40	-.36	.33	.31	.18	.07
HV IsoS	.14	.20	.16	.19	.41	.29	.33	.41	-.12	-.46	-.51	-.46	.39	.39	.22	.07
JD Lum	-.06	-.18	.04	.07	.26	.23	.17	.03	-.24	-.12	-.11	-.04	.25	.11	-.06	-.02
JD LumLow	-.01	-.17	.04	.19	.29	.30	.22	.14	-.36	-.01	.00	.02	.21	.18	-.05	-.03
JD Iso	.18	.07	.19	.28	.27	.26	.17	.04	-.28	-.20	-.13	.06	.54	.52	.41	.46
JD IsoS	.01	-.09	.06	.18	.46	.39	.40	.27	-.15	-.05	.02	.01	.24	.21	-.05	.08
ML Lum	.74	.92	.90	.86	.27	.18	.18	.27	.18	-.20	-.18	-.13	.22	.41	.05	.13
ML LumLow	1	.65	.90	.84	.24	.06	.15	.23	.30	-.23	-.17	-.16	.24	.34	.05	.07
ML Iso	1	1	.77	.93	.24	.08	.16	.26	.12	-.25	-.12	-.18	.15	.26	-.08	-.05
ML IsoS	1	1	1	.65	.18	.04	.10	.21	.10	-.20	-.07	-.16	.30	.39	.07	.02
PD Lum	.44	.41	.38	.32	.52	.89	.86	.86	-.04	-.12	-.14	-.08	.20	.32	-.15	.09
PD LumLow	.30	.11	.13	.07	1	.47	.93	.87	-.10	-.09	-.13	.01	.21	.32	.00	.20
PD Iso	.27	.24	.24	.17	1	1	.59	.91	.05	.00	.03	.10	.11	.25	-.08	.11
PD IsoS	.45	.42	.43	.39	1	1	1	.48	-.04	-.16	-.15	-.16	.12	.27	-.12	.06
PZ Lum	.32	.56	.21	.17	-.08	-.22	.09	-.08	.46	.63	.49	.53	.12	.06	.00	.08
PZ LumLow	-.34	-.43	-.43	-.37	-.25	-.19	.00	-.35	1	.45	.87	.90	-.09	.04	-.06	.06
PZ Iso	-.29	-.30	-.19	-.12	-.27	-.26	.06	-.32	1	1	.51	.84	-.15	-.03	-.08	.05
PZ IsoS	-.19	-.24	-.26	-.25	-.14	.02	.15	-.28	.97	1	1	.66	.07	.18	.16	.31
ZN Lum	.35	.39	.23	.50	.37	.41	.19	.22	.23	-.17	-.29	.12	.57	.84	.81	.69
ZN LumLow	.68	.61	.43	.70	.65	.68	.46	.56	.14	.08	-.06	.33	1	.48	.76	.74
ZN Iso	.12	.14	-.18	.18	-.45	.00	-.23	-.39	.00	-.18	-.23	.43	1	1	.22	.81
ZN IsoS	.33	.19	-.12	.04	.26	.61	.30	.18	.26	.19	.15	.81	1	1	1	.23

Table 2. Diagonal (in gray): Intrarater reliability expressed as intraclass correlation coefficients ($ICC_{3,1}$) for each condition. Upper triangle: Attenuated correlation coefficients between each pair of conditions (Bravais–Pearson's *r*). Lower triangle: Disattenuated correlation coefficients between each pair of conditions (Bravais–Pearson's *r*). Italics and bold font indicate significant results without and with Bonferroni correction, respectively. The color scale from blue to red reflects effect sizes from $r = -1$ to $r = 1$ (white corresponds to $r = 0$). Intra-illusion correlations are strong while inter-illusion correlations are in general weaker. The BS and HV illusions correlated strongly.

8%; RF9: 7%) and are closely related to nine illusion types, each of them containing all four different luminance conditions (Table 3). The BS and HV illusions loaded on the same factor (RF1). In the unrotated factor solution, the first factor accounted for about 27% of the total variance.

Data simulation

Based on the intra-illusion correlation coefficients observed in Experiment 1 ($M = 0.43$, $SD = 0.12$), we simulated normally distributed intra-illusion correlation coefficients. Individual mean adjustments were simulated from a normal distribution ($M = 0$,

		RF1	RF2	RF5	RF3	RF4	RF6	RF8	RF7	RF9
BS	**Lum**	0.90	−0.02	−0.12	−0.08	0.12	−0.15	0.05	−0.05	−0.07
BS	**LumLow**	0.89	0.09	−0.08	−0.18	0.07	−0.06	0.04	−0.09	0.14
BS	**Iso**	0.90	0.02	0.11	−0.03	0.05	−0.12	0.15	0.02	−0.01
BS	**IsoS**	0.91	−0.08	−0.01	−0.21	0.00	−0.11	0.10	−0.01	0.19
DB	**Lum**	0.09	0.95	−0.10	−0.15	0.00	0.01	−0.03	0.01	0.02
DB	**LumLow**	0.07	0.90	0.06	−0.06	−0.05	−0.02	−0.01	0.02	0.15
DB	**Iso**	−0.05	0.92	0.08	0.05	0.00	0.03	−0.08	−0.05	0.06
DB	**IsoS**	−0.06	0.97	0.06	0.15	−0.03	−0.05	−0.04	−0.06	−0.04
EH	**Lum**	−0.03	0.00	−0.12	0.91	0.04	−0.13	0.13	−0.14	0.02
EH	**LumLow**	−0.04	−0.27	0.01	0.82	−0.02	0.01	−0.04	−0.06	0.11
EH	**Iso**	0.08	0.07	−0.02	0.75	0.06	0.01	0.10	0.17	−0.02
EH	**IsoS**	0.05	0.23	−0.07	0.86	−0.08	0.12	−0.08	−0.07	0.06
HN	**Lum**	−0.05	−0.12	−0.08	0.11	0.21	0.78	−0.10	−0.07	0.26
HN	**LumLow**	0.06	0.03	0.02	0.10	−0.03	0.97	0.11	0.07	−0.13
HN	**Iso**	−0.13	−0.04	−0.01	0.04	0.01	0.86	−0.07	0.02	0.04
HN	**IsoS**	0.09	0.11	0.12	−0.27	−0.03	0.79	0.14	−0.13	0.10
HV	**Lum**	0.90	0.03	0.06	0.18	−0.10	−0.01	0.09	−0.05	−0.09
HV	**LumLow**	1.01	−0.08	0.03	0.24	−0.09	0.09	−0.11	0.11	−0.09
HV	**Iso**	1.00	0.08	−0.08	0.06	−0.06	0.18	−0.02	0.06	−0.10
HV	**IsoS**	0.88	−0.01	−0.05	0.17	0.07	0.11	−0.09	−0.10	−0.05
JD	**Lum**	0.20	−0.31	0.00	0.03	−0.12	−0.02	0.80	−0.01	0.03
JD	**LumLow**	−0.19	−0.16	0.12	0.16	0.06	−0.09	0.84	−0.07	−0.09
JD	**Iso**	0.03	0.16	0.08	0.10	−0.09	0.00	0.84	−0.05	0.29
JD	**IsoS**	0.17	0.07	−0.07	−0.11	0.12	0.14	0.86	0.11	−0.08
ML	**Lum**	−0.09	0.09	0.97	0.04	0.11	−0.16	−0.02	−0.02	0.02
ML	**LumLow**	0.07	0.06	0.94	−0.01	0.03	−0.04	−0.18	0.04	−0.02
ML	**Iso**	−0.03	−0.05	0.99	−0.11	−0.02	0.06	0.10	−0.03	−0.10
ML	**IsoS**	−0.09	−0.03	0.96	0.00	−0.10	0.19	0.20	−0.02	−0.10
PD	**Lum**	0.09	0.14	0.10	0.10	0.88	−0.10	0.10	0.01	−0.17
PD	**LumLow**	−0.11	−0.07	−0.07	0.06	1.00	−0.04	0.04	−0.08	0.12
PD	**Iso**	0.06	−0.09	−0.06	−0.10	0.93	0.16	0.03	0.14	−0.01
PD	**IsoS**	0.02	−0.04	0.07	−0.02	0.93	0.10	−0.13	−0.08	−0.09
PZ	**Lum**	0.21	−0.09	0.19	−0.08	−0.03	0.00	−0.29	0.74	0.07
PZ	**LumLow**	−0.07	−0.02	−0.09	0.07	0.01	−0.15	0.01	0.93	−0.04
PZ	**Iso**	−0.21	0.11	−0.06	0.00	−0.04	0.18	0.17	0.83	−0.22
PZ	**IsoS**	−0.14	−0.03	−0.11	−0.02	0.03	−0.07	0.15	0.88	0.25
ZN	**Lum**	0.10	−0.14	0.14	0.40	−0.03	0.08	0.03	0.02	0.62
ZN	**LumLow**	0.05	0.11	0.27	0.52	0.15	−0.07	0.00	0.12	0.44
ZN	**Iso**	0.01	0.01	−0.12	0.32	−0.19	0.11	−0.10	−0.03	0.80
ZN	**IsoS**	−0.14	0.33	−0.16	0.13	0.09	0.01	0.12	0.11	0.73

Table 3. Rotated factor loadings from an exploratory factor analysis (EFA) after promax rotation for all illusions and orientations. A color scale from blue (negative loadings) to red (positive loadings) is shown.

$SD = 1$) and inter-illusion correlation coefficients were computed from these simulated values. The probability of observing less than 100% of intra-illusion and more than 27% of inter-illusion correlation coefficients larger than 0.3 across 10,000 simulations was null, since it never happened that more than 27% of simulated inter-illusion correlations showed $r > 0.3$. On average, 15% and 86% of simulated inter- and intra-illusion correlation coefficients were larger than 0.3, respectively, suggesting that we may underestimate the true inter- and intra-illusion effect sizes.

Importantly, a strongly significant difference was observed when computing a Welch t test between the observed inter- and intra-illusion correlation coefficients (two-tailed t test, $t[110.46] = 40.81$, $p < 0.001$), suggesting a true difference between inter- and intra-illusion correlations despite the small sample size and the very large number of comparisons.

Experiment 3

In the first experiment, we observed that individual differences in visual illusions are not specific to features such as color, shape, or texture. The second experiment suggested that individual differences in visual illusions are not specific to luminance changes. In addition, there were only very weak associations between different visual illusions, except between the BS illusion and the HV illusion (see also Hamburger & Hansen, 2010), which is in fact a BS illusion rotated by 90°. We here tested whether individual differences for visual illusions are stable across changes in orientation.

Methods

Participants

Twenty students of the EPFL participated in this experiment (seven females, mean age: 23 years, age range: 18–28 years). Participants signed informed consent prior to the experiment and were paid 20 Swiss Francs per hour. Procedures were conducted in accordance with the Declaration of Helsinki except for the pre-registration (§ 35) and were approved by the local ethics committee.

Apparatus

The same experimental setup as in Experiment 1 was used except that the experiment was conducted in the Laboratory of Psychophysics at EPFL, Switzerland.

Stimuli

Five illusions were tested: horizontal-vertical (HV), Müller-Lyer (ML), Poggendorff (PD), Ponzo (PZ) and Zöllner (ZN). Stimuli were presented in white ($\approx$ 176 cd/m^2) on a black background ($\approx$ 1 cd/m^2). In the HV, ML, and PZ illusions, participants had to adjust the length of a target line to match the length of a reference line by moving the computer mouse on the horizontal axis. In the PD, the right part of the interrupted diagonal had to be vertically adjusted along the right parallel line by moving the computer mouse from left to right so that it appeared to be in a continuum with the left part of the interrupted diagonal. In the ZN illusion, moving the mouse on the horizontal axis changed the alignment of the main streams (two neighbor streams always bent in opposite directions). Participants validated the trial when they perceived these main streams to be perfectly parallel. All lines were drawn with a 4-pixel width.

Each illusion was presented under four different orientations: −60°, −15°, 30°, and 75° (Figure 8). Illusions are described in detail in Supplementary File S1.

Procedure

The experimenter first explained the task to the participants who adjusted each illusion in the 0° orientation for one trial to familiarize with the task. Then, each of the 20 conditions (5 illusions $\times$ 4 orientations) was presented twice without time restriction. The two trials for each condition were presented sequentially, i.e., one after the other, but the order of the 20 conditions was randomized across participants.

As in Experiment 1, participants were asked to perform the task relying on their percepts only. Participants could ask questions at any time since the experimenter stayed in the experimental room during the whole experiment. Contrary to Experiment 1, participants were not shown their own results at the end of the experiment.

Data analysis

For each participant and each condition, the adjustments from both trials were averaged. Then, the reference value of each condition was subtracted from the averaged values. In order to make the scores comparable across illusions, illusion magnitudes were turned into modified z-scores for illusion type. No outliers were detected based on the same outlier detection method as in Experiments 1 and 2. A repeated-measures ANOVA with two main factors (illusion and orientation) was computed. Similarly to Experiment 2, we computed intrarater reliabilities as well as a correlation table with both attenuated and disattenuated correlation coefficients and an EFA with an oblique rotation method (promax).

Results

Magnitudes of the illusions

Standardized illusion magnitudes are plotted for each illusion and each orientation in Figure 9. A repeated-measures ANOVA was computed with the main factors of illusion (HV, ML, PD, PZ, ZN) and orientation (−60°, −15°, 30°, and 75°). There was a significant interaction ($F[12, 228] = 3.996$, $p < 0.001$, $\eta_p^2 = 0.174$) and a significant main effect of orientation

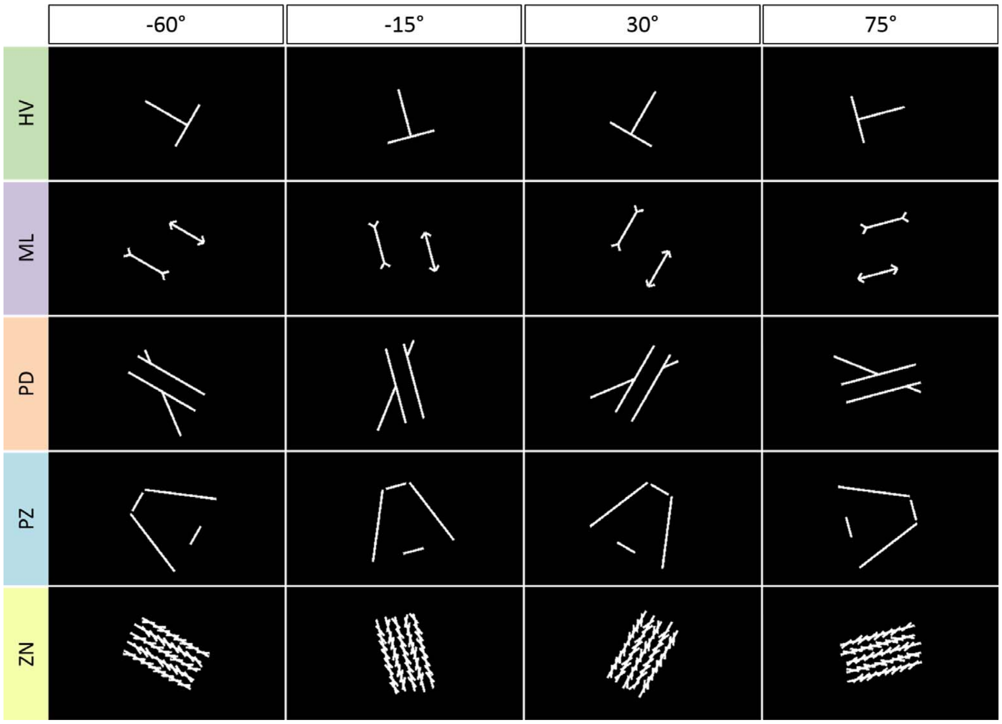

Figure 8. The five illusions used in Experiment 3, tested with four different orientations. By row: horizontal-vertical (HV), Müller-Lyer (ML), Poggendorff (PD), Ponzo (PZ), and Zöllner (ZN) illusions. By column: −60°, −15°, 30°, and 75°. In the HV, ML, and PZ illusions, participants adjusted the length of a line to match the length of a reference line. In the PD illusion, participants adjusted the position of the right part of the interrupted diagonal so that it appeared to be in a continuum with the left part. In the ZN illusion, participants aligned the five main streams in a parallel way. All adjustments were made by moving the computer mouse on the horizontal axis. Each condition was presented twice and the order of presentation was randomized across participants.

($F[3, 57] = 13.827$, $p < 0.001$, $\eta_p^2 = 0.421$). There was no main effect of illusion ($p = 0.880$).

Intrarater reliability

Intraclass correlations ($ICC_{3,1}$) were computed between the first and second adjustments of all participants for each condition (Table 4, diagonal). Five out of 20 intraclass correlations were not significant after Bonferroni correction but yielded significance without correction, suggesting an overall moderate intrarater reliability (PD −15°: ICC coef. = 0.546, 95% CI [0.148, 0.792], $F[19, 19] = 3.405$, $p = 0.005$; PZ 30°: ICC coef. = 0.438, 95% CI [0.006, 0.732], $F[19, 19] = 2.559$, $p = 0.023$; PZ 75°: ICC coef. = 0.431, 95% CI [0.000, 0.728], $F[19, 19] = 2.517$, $p = 0.025$; ZN −60°: ICC coef. = 0.396, 95% CI [0.000, 0.708], $F[19, 19] = 2.311$, $p = 0.038$; ZN −15°: ICC coef. = 0.494, 95% CI [0.077, 0.763], $F[19, 19] = 2.950$, $p = 0.011$).

Correlations between illusion magnitudes

Attenuated (Table 4, upper triangle) and disattenuated (Table 4, lower triangle) correlation coefficients were reported both without and with Bonferroni correction. Among 190 correlations, 55 attenuated and 81 disattenuated correlations resulted in $r > 0.3$. Interestingly, 97% (29 out of 30) and 100% of the attenuated and disattenuated intra-illusion correlations showed $r > 0.3$, respectively. In contrast, only 16% (26 out of 160) and 32% (51 out of 160) of the attenuated and disattenuated inter-illusion correlations showed $r > 0.3$, respectively (Figure 10). Hence, it seems that intra-illusion correlations were stronger than inter-illusion correlations, even though intrarater reliabilities were not always high.

Exploratory factor analysis (EFA)

We conducted an exploratory factor analysis with an oblique rotation. We identified four factors by scree plot inspection, which accounted for ~61% of the variability of the data (RF1: 17%, RF2: 17%, RF3: 15%, RF4: 12%). In the unrotated factor solution, the first factor explained about 22% of the total variance. Rotated factor loadings are presented in Table 5. The first factor was mainly composed of the PD and ZN conditions while the second factor mainly loaded on the HV and PD conditions. The third and fourth factors were respectively dominated by loadings from the ML and PZ conditions. Each illusion mainly loaded on one

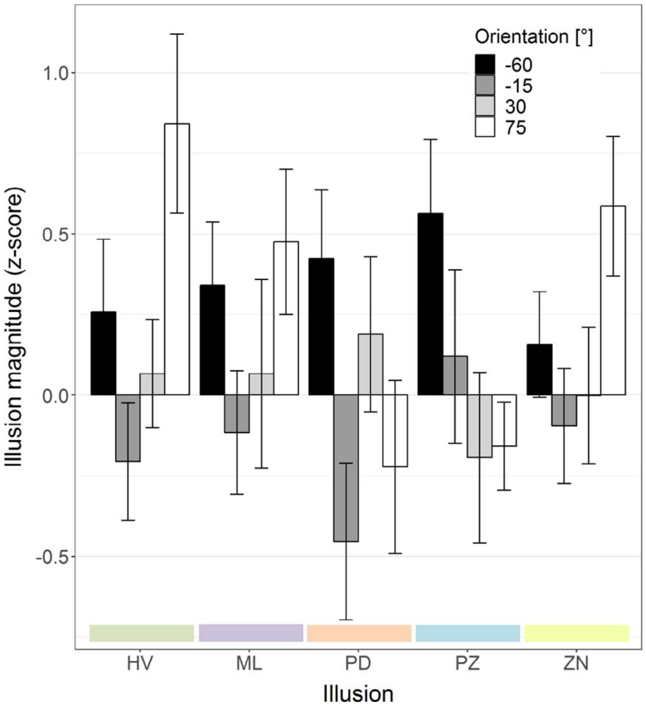

Figure 9. Standardized illusion magnitudes ± *SEM* as a function of the orientation [°] for each illusion. The *z*-scores show to what extent the illusion magnitudes deviate as a function of orientation for each illusion type.

factor, except for the PD conditions which highly loaded on two (or three) factors.

Data simulation

As in Experiment 2, we simulated intra-illusion correlation coefficients from the effect size observed in

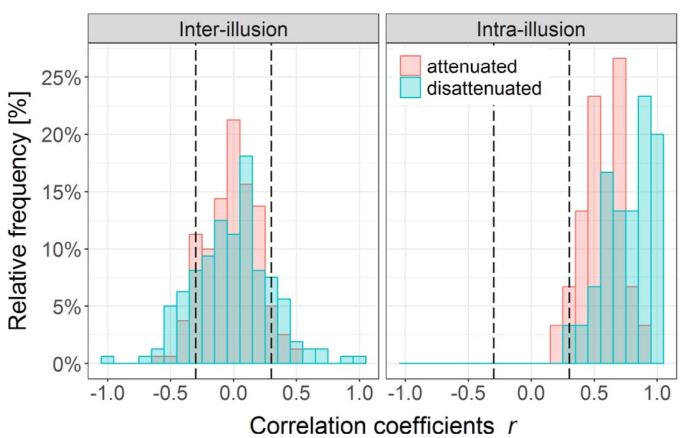

Figure 10. Relative frequency (in percentage) of attenuated (red) and disattenuated (turquoise) correlation coefficients *r* for inter- (left panel) and intra-illusion (right panel) correlations in Experiment 3. According to Cohen's convention (Cohen, 1988), *r* = ±0.3 (vertical dashed lines) is the lower limit corresponding to a medium effect size.

Experiment 1, while inter-illusion correlation coefficients were computed from simulated data with $M = 0$ and $SD = 1$. The probability of observing less than 97% of intra-illusion and more than 16% of inter-illusion correlation coefficients across 10,000 simulations was 89%. Indeed, there were on average 20% of inter- and 86% of intra-illusion correlation coefficients larger than 0.3, suggesting that we may underestimate the true intra-illusion effect size.

A Welch t test between the observed inter- and intra-illusion correlation coefficients resulted in a strongly significant difference (two-tailed t test, $t[48.37] = 17.37$, $p < 0.001$), highlighting a difference between inter- and intra-illusion correlations despite the small sample size.

Discussion

Previous research did not find evidence for a common factor for visual illusions (Grzeczkowski et al., 2017; Grzeczkowski et al., 2018). Here, we systematically examined hyper-specificity of factors for visual illusions. We especially wondered whether these factors are as specific as in perceptual learning. To this end, we presented several variants of different visual illusions. We observed strong correlations between the different variants of each illusion (intra-illusion correlations) but only weak correlations between different illusions (inter-illusion correlations), which suggests that factors are illusion-specific.

In Experiment 1, we tested different variants of the Ebbinghaus illusion and found high correlations between the illusion magnitudes of the different variants. For example, illusion magnitudes significantly correlated between the STD (standard) and the FRT (fast rotating flankers) conditions (Figure 1). These results suggest one mechanism behind the Ebbinghaus illusion, corroborated by a factor analysis showing evidence for only one main factor. A similar result was previously found for the Müller-Lyer illusion (Coren, Girgus, Erlichman, & Hakstian, 1976). A factor analysis showed that 45 measures of different illusions were best represented by a two-factor model, with one factor mainly loading on several variants of the Müller-Lyer illusion.

In Experiment 2, we reanalyzed a dataset, in which 10 different illusions were tested with four luminance conditions. We found high intra-illusion correlations for different luminance conditions, but weak inter-illusion correlations. However, the BS illusion magnitudes strongly correlated with the HV illusion magnitudes. In fact, the HV illusion is a BS illusion rotated by 90°. An EFA identified nine main components which explained ~90% of the variance. Strikingly, each

	HV -60	HV -15	HV 30	HV 75	ML -60	ML -15	ML 30	ML 75	PD -60	PD -15	PD 30	PD 75	PZ -60	PZ -15	PZ 30	PZ 75	ZN -60	ZN -15	ZN 30	ZN 75
HV -60	***.74***	.43	*.50*	*.71*	−.13	.12	.05	−.35	.08	−.08	−.18	−.17	.07	.04	.15	.06	−.08	.07	−.12	−.04
HV -15	*.55*	***.86***	*.61*	*.73*	−.06	.05	−.25	−.31	−.35	−.31	−.09	−.28	−.19	−.13	−.15	.01	−.06	.15	.04	.22
HV 30	*.72*	***.80***	***.66***	*.71*	.10	.00	−.13	−.33	*−.45*	−.31	−.40	−.26	.02	.04	.21	*.51*	.03	.16	.05	−.05
HV 75	***.85***	***.81***	***.90***	***.94***	.13	.23	.06	−.29	−.22	−.30	−.28	−.38	.01	.16	.11	0.11	−.03	.10	−.06	.05
ML -60	−.17	−.07	.14	.14	***.83***	*.72*	*.60*	*.52*	−.18	−.17	−.30	−.29	.12	.27	.11	.01	.01	−.01	.07	−.08
ML -15	.15	.06	.00	.26	***.85***	***.85***	***.79***	.39	−.09	−.11	−.17	−.24	.25	.38	.24	−.02	.23	.18	.18	−.02
ML 30	.06	−.28	−.16	.06	*.69*	***.89***	***.91***	*.55*	−.01	−.06	−.10	−.25	.11	.15	.17	−.11	.33	.16	.08	−.08
ML 75	*−.46*	−.37	*−.45*	−.34	*.63*	*.47*	*.64*	***.81***	.02	.15	.13	.08	−.11	−.06	.03	−.37	.33	.23	.29	.41
PD -60	.10	−.40	*−.59*	−.25	−.21	−.11	−.01	.03	***.87***	*.45*	*.55*	*.58*	.21	.11	−.01	−.26	.23	.08	.18	−.04
PD -15	−.12	*−.45*	*−.51*	−.42	−.25	−.16	−.08	.23	*.65*	*.55*	*.71*	*.70*	−.13	−.33	−.03	.00	*.47*	.16	.19	.01
PD 30	−.22	−.10	*−.52*	−.31	−.36	−.20	−.12	.16	*.64*	***1***	***.85***	***.78***	−.26	−.35	−.43	−.30	.40	.31	.32	.25
PD 75	−.21	−.33	−.34	−.41	−.34	−.28	−.28	.09	*.66*	***1***	***.90***	***.88***	.04	−.21	−.22	.05	.41	.20	.34	.06
PZ -60	.09	−.25	.04	.01	.16	.32	.14	−.14	.26	−.21	−.33	.05	***.73***	*.54*	*.52*	*.47*	.04	−.03	.04	−.22
PZ -15	.06	−.16	.06	.20	.35	*.48*	.18	−.08	.14	*−.53*	*−.45*	−.27	***.74***	***.72***	*.50*	.19	−.16	−.24	−.15	.04
PZ 30	.27	−.24	.38	.18	.18	.40	.27	.05	−.02	−.06	*−.70*	−.36	***.93***	***.89***	*.44*	*.57*	.03	−.04	.07	−.25
PZ 75	.10	.02	***.95***	.18	.02	−.03	−.17	*−.63*	−.42	.00	*−.49*	.09	***.83***	.35	***1***	*.43*	−.06	−.18	−.07	*−.56*
ZN -60	−.14	−.10	.06	−.04	.02	.40	*.56*	*.58*	.39	***1***	*.69*	*.69*	.07	−.30	.06	−.13	*.40*	***.74***	*.69*	.31
ZN -15	.12	.23	.27	.14	−.02	.27	.24	.37	.13	.31	*.47*	.31	−.04	−.41	−.09	−.40	***1***	*.49*	***.92***	.44
ZN 30	−.15	.05	.06	−.07	.09	.22	.10	.36	.21	.29	.39	.41	.05	−.20	.12	−.12	***1***	***1***	***.79***	.31
ZN 75	−.05	.28	−.07	.07	−.11	−.02	−.11	*.55*	−.05	.01	.33	.08	−.31	.06	*−.46*	***−1***	*.59*	***.76***	.43	***.68***

Table 4. Diagonal (in gray): Intrarater reliability expressed as intraclass correlation coefficients ($ICC_{3,1}$) for each condition. Upper triangle: Attenuated correlation coefficients between each pair of conditions (Bravais–Pearson's r). Lower triangle: Disattenuated correlation coefficients between each pair of conditions (Bravais–Pearson's r). Italics and bold font indicate significant results without and with Bonferroni correction, respectively. The color scale from blue to red reflects effect sizes from $r = -1$ to $r = 1$ (white corresponds to $r = 0$).

component mainly loaded on one illusion except for the BS and HV illusions, which highly loaded on the same component.

The strong correlations between the four luminance conditions indicate that, contrary to a widely held belief (e.g., Livingstone & Hubel, 1987), visual illusions do not break down under conditions of isoluminance and are therefore not primarily processed by the magnocellular system (also after controlling for subjective isoluminance, cf. Hamburger et al., 2007).

In Experiment 3, five visual illusions were tested with four orientations. Again, intra-illusion correlations were mostly high, while inter-illusion correlations were mostly weak. Hence, we found almost no significant inter-illusion correlations in both Experiments 2 and 3, as observed in Grzeczkowski et al. (2017). Furthermore, in all three experiments, a dimensionality reduction technique (EFA) showed that more or less each illusion makes up its own factor. The PD illusion loaded on only one factor in Experiment 2 but was related to the HV, ML, and ZN illusions in Experiment 3, which may be due to chance.

In Experiment 2, we found no link between the EH and DB illusions, which are often proposed to rely on the same mechanism (Coren et al., 1976; Girgus, Coren, & Agdern, 1972; Roberts, Harris, & Yates, 2005). Likewise, there was no link between the JD and ML illusions. An explanation may be that the two segments compared in the JD illusion are collinear while on top of each other in the ML illusion. The absence of significant correlations between the EH and DB illusions is, however, more puzzling. However, it is important to note that we are not making conclusions on specific comparisons in this study such as the comparison between the EH and DB illusion. For such a purpose, we do not have sufficient power. The

	RF1	RF2	RF3	RF4
HV -60	0.12	0.59	−0.14	0.12
HV -15	0.09	0.86	−0.19	−0.27
HV 30	0.17	0.90	−0.15	0.21
HV 75	0.12	0.87	0.01	0.03
ML -60	−0.03	−0.07	0.76	0.06
ML -15	0.21	0.05	0.82	0.18
ML 30	0.16	−0.16	0.82	0.08
ML 75	0.21	−0.40	0.70	−0.26
PD -60	0.33	−0.37	−0.13	0.16
PD -15	0.49	−0.32	−0.20	0.08
PD 30	0.53	−0.28	−0.27	−0.24
PD 75	0.57	−0.33	−0.37	0.14
PZ -60	0.12	−0.05	0.15	0.71
PZ -15	−0.14	−0.04	0.29	0.44
PZ 30	0.11	0.08	0.21	0.72
PZ 75	0.05	0.22	−0.21	0.77
ZN -60	0.90	0.11	0.25	0.07
ZN -15	0.90	0.38	0.21	−0.12
ZN 30	0.85	0.20	0.21	0.02
ZN 75	0.29	0.14	0.15	−0.47

Table 5. Rotated factor loadings from an exploratory factor analysis (EFA) after promax rotation for all illusions and orientations. A color scale from blue (negative loadings) to red (positive loadings) is shown.

purpose of this study was to show that *in general* variants of one illusion type show strong correlations but inter-illusion correlations are weak(er). It is the data as a whole which is important and not single, specific findings.

Perceptual learning is usually very specific to the trained stimuli. For example, when a Vernier offset discrimination task is trained, performance improves. However, learning transfers only when the Vernier is rotated up to 10° (Spang et al., 2010) but not when rotated by 90° (Ball & Sekuler, 1987; Fahle & Morgan, 1996; Schoups et al., 1995). However, we found high correlations when illusions were rotated by −60°, −15°, 30°, and 75° (Experiment 3). In Experiment 2, the BS illusion strongly correlated with the HV illusion, which is just the BS illusion rotated by 90°. Hence, factors for illusions are not as specific as one may have expected from perceptual learning, where learning is usually retinotopic and orientation-specific. Therefore, perceptual learning does not seem to shape the factors underlying visual illusions, as long as everyday perceptual learning is as specific as under laboratory conditions (just to mention, transfer of perceptual learning in the laboratory can occur; e.g., Aberg, Tartaglia, & Herzog, 2009).

In Experiment 1, we expected the control condition (CON) to show a null effect, which however was not the case. We suggest that our procedure induced a bias. The adjustable target was always surrounded by larger flankers compared to the reference target. Since participants overadjusted the size of the target in each noncontrol condition, we suggest that it induced a small but significant bias in the control condition as well. We hypothesize that this bias would disappear if the adjustable target was randomly surrounded by large or small flankers. Illusion magnitudes varied as a function of the size of the flankers, as highlighted by the FBIG and FSMA conditions, where we observed larger and smaller effects compared to the STD condition, respectively. The size of the flankers can indeed influence illusion magnitudes (e.g., Roberts et al., 2005).

We reported significance both without correction and with the very conservative Bonferroni correction, since we sometimes aimed for null results and sometimes not. Therefore, we considered the most extreme option in each case. In Experiment 1, correlations were significant even when the alpha level was corrected for family-wise errors. In Experiments 2 and 3, inter-illusion correlations were mostly nonsignificant even though we did not correct the alpha level for multiple comparisons and intra-illusion correlations were mostly significant both without and with Bonferroni correction.

Intrarater reliabilities were mostly significant but moderate, reflecting a nonnegligible within-participant variation that can be explained by the low number of repetitions per condition and by measurement errors. This may put an upper limit on the observed pairwise correlations, i.e., it may lead to underestimated correlations (Bosten et al., 2017; Mollon, Bosten, Peterzell, & Webster, 2017). To account for this, we computed disattenuated correlations. Similar patterns of correlations were observed between attenuated and disattenuated correlations (see Tables 1, 2, and 4). Hence, our null results are unlikely to be type II errors. Moreover, a Bayesian approach previously showed that the null hypothesis was more likely than the alternative hypothesis for inter-illusion correlations with significant intrarater reliabilities (Grzeczkowski et al., 2017). Intrarater reliabilities were higher in Experiment 2 than in Experiment 1, likely because we had four instead of two trials per condition, respectively. We like to mention that between-condition variations may be higher than within-condition variations in Experiments 1 and 3, since both trials of a condition were always presented sequentially, i.e., one after the other, which may inflate intrarater reliabilities.

Power may be an issue, especially in Experiments 2 and 3, in which we had small sample sizes. Data simulation in Experiment 3 resulted in a high likelihood of observing a smaller percentage of intra-illusion correlation coefficients and a larger percentage of inter-illusion correlation coefficients larger than 0.3 compared to what we actually observed. On the contrary, this likelihood was null in Experiment 2. Indeed, the proportion of simulated inter-illusion correlations with $r > 0.3$ never reached the 27% observed in the data, which suggests that the true inter-illusion effect size is nonnull. The average proportion of simulated intra-illusion coefficients larger than 0.3 was 86%, while all observed intra-illusion correlations showed $r > 0.3$, indicating that we may also underestimate the true intra-illusion effect size.

Importantly, there are strong differences between the inter- and intra-illusion correlation coefficients in Experiments 2 and 3, supporting our claim. In addition, we like to mention that we observed significant correlation coefficients both without and with the conservative Bonferroni correction.

Often illusions are implicitly or explicitly classified according to certain criteria, such as their geometric-spatial features, and it is assumed that a common mechanism is in operation (e.g., Coren et al., 1976; Ninio, 2014; Piaget, 1961). Our study cannot address the question of which mechanisms are at work but challenges the notion that there are common explanations for classes of illusions (for a critical review see Hamburger, 2016).

The Ebbinghaus illusion magnitude was shown to negatively correlate with V1 cortex size (de Haas, Kanai, Jalkanen, & Rees, 2012; Schwarzkopf & Rees, 2013; Schwarzkopf, Song, & Rees, 2011). However, whether this conclusion extends to other visual illusions may be questioned given the large individual differences we found. Our experiments tested a battery of illusions rather than investigating the mechanisms of one illusion as is common practice (but see Coren et al., 1976; Thurstone, 1944). The factor structure is not only sparse for illusions but also for vision in general. For example, a distinct factor structure was found for contrast: sensitivities correlated between 0.2 and 0.4 c/°, between 0.4 and 1.2 c/° and between 1.2 to 3 c/°, but correlations were weak between these different ranges (Peterzell, 2016; Peterzell, Schefrin, Tregear, & Werner, 2000). Similarly, Emery and colleagues (2017a, 2017b) observed several small factors underlying individual differences in hue scaling. In addition, Bosten and Mollon (2010) found "no noteworthy general trait of susceptibility" (p. 1663) for contrast perception. When comparing different spatial tasks, such as bisection discrimination and Vernier offset discrimination, only low correlations were found (Cappe et al., 2014). Likewise, there was little evidence for a common factor for oculomotor tasks (Bargary et al., 2017) and for binocular rivalry and other bistable paradigms (Brascamp et al., 2018; Cao et al., 2018; Wexler, 2005). Chamberlain, Van der Hallen, Huygelier, Van de Cruys, and Wagemans (2017) also showed poor evidence for a common factor for local and global visual processing. In addition, the effects of priors in perceptual tasks seem not to follow a single mechanism (Tulver, Aru, Rutiku, & Bachmann, 2019). Hence, these studies found very specific factors, similar to the very specific factors we found for visual illusions, and are rather arguing against a general factor for vision as proposed previously (e.g., Halpern, Andrews, & Purves, 1999). It appears that even studies that had a narrowly defined hypothesis by including several tasks that tap into a specific functional ability or theoretical construct of perception have often not succeeded in finding evidence to support the existence of a stable factor in perception (Tulver, 2019).

Surprisingly, whereas most inter-illusion magnitudes are only weakly correlated, there may be links between certain visual illusions. For example, Grzeczkowski and colleagues (2017, 2018) found significant correlations between the Ebbinghaus and Ponzo illusions, which we could not, however, reproduce here (Table 2, triangle) and was similarly not found by Schwarzkopf and colleagues (2011). However, the power was much higher in the studies by Grzeczkowski and colleagues (2017, 2018) than here. In addition, they also found that the Ponzo illusion magnitude correlated with cognitive disorganization. However, this was the only illusion that correlated with a personality trait. Given the large number of statistical comparisons, it may be that these few significant correlations are false positives. Alternatively, it may be that within an ocean of weak correlations there are some strong singular correlations, such as between the Ponzo illusion and cognitive organization or between two rather unrelated illusions. Whereas these links may be surprising from a vision science perspective, they may be less surprising from a genetic point of view. As a metaphor, a hypothetical gene may code for a protein, which plays an important role in the visual cortex and, say, in the liver. Variability in the gene may cause significant correlations between visual and liver functions, which may appear bizarre as long as one expects that visual functions rather than visual and liver functions go together. In this line, Frenzel et al. (2012) found correlations between auditory and touch perception as both sensory systems rely on mechanoreceptors encoded by the same gene.

In summary, common factors are ubiquitous. However, there is little evidence for a unique common factor for vision (e.g., Bosten & Mollon, 2010; Cappe et al., 2014; Coren, Girgus, & Day, 1973; Grzeczkowski et al., 2017; Peterzell, Chang, & Teller, 2000; Peterzell & Teller, 1996; Peterzell, Werner, & Kaplan, 1993, 1995; Webster & MacLeod, 1988). Here, we showed that the factor structure underlying visual illusions is sparse.

However, factors are not as specific as it may be expected from perceptual learning. It seems that most illusions make up their own factor.

Keywords: factors, illusions, individuality, perception

Acknowledgments

We thank Marc Repnow for technical support and helpful comments. This work was supported by the project "Basics of visual processing: From elements to figures" (Project number: 320030_176153 / 1) of the Swiss National Science Foundation (SNSF) and by a National Centre of Competence in Research (NCCR Synapsy) grant from the SNSF (51NF40-185897).

Commercial relationships: none.
Corresponding author: Aline F. Cretenoud.
Email: aline.cretenoud@epfl.ch.
Address: Laboratory of Psychophysics, Brain Mind Institute, École Polytechnique Fédérale de Lausanne (EPFL), Lausanne, Switzerland.

References

Aberg, K. C., Tartaglia, E. M., & Herzog, M. H. (2009). Perceptual learning with chevrons requires a minimal number of trials, transfers to untrained directions, but does not require sleep. *Vision Research*, *49*(16), 2087–2094, https://doi.org/10.1016/j.visres.2009.05.020

Axelrod, V., Schwarzkopf, D. S., Gilaie-Dotan, S., & Rees, G. (2017). Perceptual similarity and the neural correlates of geometrical illusions in human brain structure. *Scientific Reports*, *7*:39968, https://doi.org/10.1038/srep39968.

Ball, K., & Sekuler, R. (1987). Direction-specific improvement in motion discrimination. *Vision Research*, *27*(6), 953–965.

Bargary, G., Bosten, J. M., Goodbourn, P. T., Lawrance-Owen, A. J., Hogg, R. E., & Mollon, J. D. (2017). Individual differences in human eye movements: An oculomotor signature? *Vision Research*, *141*, 157–169, https://doi.org/10.1016/j.visres.2017.03.001.

Bosten, J. M., Goodbourn, P. T., Bargary, G., Verhallen, R. J., Lawrance-Owen, A. J., Hogg, R. E., & Mollon, J. D. (2017). An exploratory factor analysis of visual performance in a large population. *Vision Research*, *141*, 303–316, https://doi.org/10.1016/j.visres.2017.02.005.

Bosten, J. M., & Mollon, J. D. (2010). Is there a general trait of susceptibility to simultaneous contrast? *Vision Research*, *50*(17), 1656–1664, https://doi.org/10.1016/j.visres.2010.05.012.

Brainard, D. H. (1997). The psychophysics toolbox. *Spatial Vision*, *10*(4), 433–436.

Brascamp, J. W., Becker, M. W., & Hambrick, D. Z. (2018). Revisiting individual differences in the time course of binocular rivalry. *Journal of Vision*, *18*(7): 3, 1–20, https://doi.org/10.1167/18.7.3. [PubMed] [Article]

Cao, T., Wang, L., Sun, Z., Engel, S. A., & He, S. (2018). The independent and shared mechanisms of intrinsic brain dynamics: Insights from bistable perception. *Frontiers in Psychology*, *9*, 589, https://doi.org/10.3389/fpsyg.2018.00589.

Cappe, C., Clarke, A., Mohr, C., & Herzog, M. H. (2014). Is there a common factor for vision? *Journal of Vision*, *14*(8):4, 1–11, https://doi.org/10.1167/14.8.4. [PubMed] [Article]

Chamberlain, R., Van der Hallen, R., Huygelier, H., Van de Cruys, S., & Wagemans, J. (2017). Local-global processing bias is not a unitary individual difference in visual processing. *Vision Research*, *141*, 247–257, https://doi.org/10.1016/j.visres.2017.01.008.

Cohen, J. (1988). *Statistical power analysis for the behavioral sciences*. Hillsdale, NJ: Lawrence Erlbaum.

Coren, S., Girgus, J. S., & Day, R. H. (1973, February 2). Visual spatial illusions: Many explanations. *Science*, *179*(4072), 503–504.

Coren, S., Girgus, J. S., Erlichman, H., & Hakstian, A. R. (1976). An empirical taxonomy of visual illusions. *Perception & Psychophysics*, *20*(2), 129–137, https://doi.org/10.3758/BF03199444.

Costello, A. B., & Osborne, J. W. (2005). Best practices in exploratory factor analysis: Four recommendations for getting the most from your analysis. *Practical Assessment, Research & Education*, *10*(7), 86–99, https://doi.org/10.1.1.110.9154.

de Haas, B., Kanai, R., Jalkanen, L., & Rees, G. (2012). Grey matter volume in early human visual cortex predicts proneness to the sound-induced flash illusion. *Proceedings of the Royal Society B: Biological Sciences*, *279*(1749), 4955–4961, https://doi.org/10.1098/rspb.2012.2132.

Derrington, A. M., Krauskopf, J., & Lennie, P. (1984). Chromatic mechanisms in lateral geniculate nucleus of macaque. *The Journal of Physiology*, *357*(1), 241–265.

Emery, K. J., Volbrecht, V. J., Peterzell, D. H., &

Webster, M. A. (2017a). Variations in normal color vision. VI. Factors underlying individual differences in hue scaling and their implications for models of color appearance. *Vision Research*, *141*, 51–65, https://doi.org/10.1016/j.visres.2016.12.006.

Emery, K. J., Volbrecht, V. J., Peterzell, D. H., & Webster, M. A. (2017b). Variations in normal color vision. VII. Relationships between color naming and hue scaling. *Vision Research*, *141*, 66–75, https://doi.org/10.1016/j.visres.2016.12.007.

Fahle, M., & Morgan, M. (1996). No transfer of perceptual learning between similar stimuli in the same retinal position. *Current Biology*, *6*(3), 292–297, https://doi.org/10.1016/S0960-9822(02)00479-7.

Faivre, N., Filevich, E., Solovey, G., Kühn, S., & Blanke, O. (2018). Behavioural, modeling, and electrophysiological evidence for supramodality in human metacognition. *Journal of Neuroscience*, *38*(2), 263–277, https://doi.org/10.1523/JNEUROSCI.0322-17.2017.

Frenzel, H., Bohlender, J., Pinsker, K., Wohlleben, B., Tank, J., Lechner, S. G., . . . Lewin, G. R. (2012). A genetic basis for mechanosensory traits in humans. *PLoS Biology*, *10*(5): e1001318, https://doi.org/10.1371/journal.pbio.1001318.

Gignac, G. E., & Szodorai, E. T. (2016). Effect size guidelines for individual differences researchers. *Personality and Individual Differences*, *102*, 74–78, https://doi.org/10.1016/j.paid.2016.06.069.

Girgus, J. S., Coren, S., & Agdern, M. (1972). The interrelationship between the Ebbinghaus and Delboeuf illusions. *Journal of Experimental Psychology*, *95*(2), 453–455, https://doi.org/10.1037/h0033606.

Goodbourn, P. T., Bosten, J. M., Hogg, R. E., Bargary, G., Lawrance-Owen, A. J., & Mollon, J. D. (2012). Do different "magnocellular tasks" probe the same neural substrate? *Proceedings of the Royal Society B: Biological Sciences*, *279*(1745), 4263–4271, https://doi.org/10.1098/rspb.2012.1430.

Grzeczkowski, L., Clarke, A. M., Francis, G., Mast, F. W., & Herzog, M. H. (2017). About individual differences in vision. *Vision Research*, *141*, 282–292, https://doi.org/10.1016/j.visres.2016.10.006.

Grzeczkowski, L., Cretenoud, A., Herzog, M. H., & Mast, F. W. (2017). Perceptual learning is specific beyond vision and decision making. *Journal of Vision*, *17*(6):6, 1–11, https://doi.org/10.1167/17.6.6. [PubMed] [Article]

Grzeczkowski, L., Roinishvili, M., Chkonia, E., Brand, A., Mast, F. W., Herzog, M. H., & Shaqiri, A. (2018). Is the perception of illusions abnormal in schizophrenia? *Psychiatry Research*, *270*, 929–939, https://doi.org/10.1016/j.psychres.2018.10.063.

Halpern, S. D., Andrews, T. J., & Purves, D. (1999). Interindividual variation in human visual performance. *Journal of Cognitive Neuroscience*, *11*(5), 521–534.

Hamburger, K. (2016). Visual illusions based on processes: New classification system needed. *Perception*, *45*(5), 588–595, https://doi.org/10.1177/0301006616629038.

Hamburger, K., & Hansen, T. (2010). Analysis of individual variations in the classical horizontal-vertical illusion. *Attention, Perception & Psychophysics*, *72*(4), 1045–1052, https://doi.org/10.3758/APP.72.4.1045.

Hamburger, K., Hansen, T., & Gegenfurtner, K. R. (2007). Geometric-optical illusions at isoluminance. *Vision Research*, *47*(26), 3276–3285, https://doi.org/10.1016/j.visres.2007.09.004.

Hemphill, J. F. (2003). Interpreting the magnitudes of correlation coefficients, *58*(1), 78–79, https://doi.org/10.1037/0003-066X.58.1.78.

Iglewicz, B., & Hoaglin, D. (1993). How to detect and handle outliers. In E. F. Mykytka (Ed.), *The ASQC basic references in quality control: Statistical techniques* (Vol. 16). Milwaukee, WI: Asq Press.

Kaliuzhna, M., Stein, T., Rusch, T., Sekutowicz, M., Sterzer, P., & Seymour, K. J. (2018). No evidence for abnormal priors in early vision in schizophrenia. *Schizophrenia Research*, *210*, 245–254, https://doi.org/10.1016/j.schres.2018.12.027.

Koo, T. K., & Li, M. Y. (2016). A guideline of selecting and reporting intraclass correlation coefficients for reliability research. *Journal of Chiropractic Medicine*, *15*(2), 155–163, https://doi.org/10.1016/j.jcm.2016.02.012.

Krauskopf, J., Williams, D. R., & Heeley, D. W. (1982). Cardinal directions of color space. *Vision Research*, *22*(9), 1123–1131.

Livingstone, M. S., & Hubel, D. H. (1987). Psychophysical evidence for separate channels for the perception of form, color, movement, and depth. *Journal of Neuroscience*, *7*(11), 3416–3468.

Mollon, J. D., Bosten, J. M., Peterzell, D. H., & Webster, M. A. (2017). Individual differences in visual science: What can be learned and what is good experimental practice? *Vision Research*, *141*, 4–15, https://doi.org/10.1016/j.visres.2017.11.001.

Ninio, J. (2014). Geometrical illusions are not always where you think they are: A review of some classical and less classical illusions, and ways to describe them. *Frontiers in Human Neuroscience*, *8*, 856, https://doi.org/10.3389/fnhum.2014.00856.

Osborne, J. W. (2003). Effect sizes and the disattenuation of correlation and regression coefficients: Lessons from educational psychology. *Practical Assessment, Research and Evaluation*, *8*(11), 5–11.

Pelli, D. G. (1997). The VideoToolbox software for visual psychophysics: Transforming numbers into movies. *Spatial Vision*, *10*, 437–442.

Peterzell, D. H. (2016). Discovering sensory processes using individual differences: A review and factor analytic manifesto. *Electronic Imaging*, *2016*(16), 1–11, https://doi.org/10.2352/ISSN.2470-1173.2016.16HVEI-112.

Peterzell, D. H., Chang, S. K., & Teller, D. Y. (2000). Spatial frequency tuned covariance channels for red-green and luminance- modulated gratings: Psychophysical data from human infants. *Vision Research*, *40*(4), 431–444, https://doi.org/10.1016/S0042-6989(99)00188-1.

Peterzell, D. H., Schefrin, B. E., Tregear, S. J., & Werner, J. S. (2000). Spatial frequency tuned covariance channels underlying scotopic contrast sensitivity. In *Vision science and its applications: OSA Technical Digest*. Washington, DC: Optical Society of America.

Peterzell, D. H., Serrano-Pedraza, I., Widdall, M., & Read, J. C. A. (2017). Thresholds for sine-wave corrugations defined by binocular disparity in random dot stereograms: Factor analysis of individual differences reveals two stereoscopic mechanisms tuned for spatial frequency. *Vision Research*, *141*, 127–135, https://doi.org/10.1016/j.visres.2017.11.002.

Peterzell, D. H., & Teller, D. Y. (1996). Individual differences in contrast sensitivity functions: The lowest spatial frequency channels. *Vision Research*, *36*(19), 3077–3085, https://doi.org/10.1016/0042-6989(96)00061-2.

Peterzell, D. H., Werner, J. S., & Kaplan, P. S. (1993). Individual differences in contrast sensitivity functions: The first four months of life in humans. *Vision Research*, *33*(3), 381–396, https://doi.org/10.1016/0042-6989(93)90093-C.

Peterzell, D. H., Werner, J. S., & Kaplan, P. S. (1995). Individual differences in contrast sensitivity functions: Longitudinal study of 4-, 6- and 8-month-old human infants. *Vision Research*, *35*(7), 961–979, https://doi.org/10.1016/0042-6989(94)00117-5.

Piaget, J. (1961). *Les mécanismes perceptifs, modèles probabilistes, analyse génétique, relations avec l'intelligence* [The mechanisms of perception] (2nd ed.). Paris, France: Presses universitaires de France.

Preacher, K. J., Zhang, G., Kim, C., & Mels, G. (2013). Choosing the optimal number of factors in exploratory factor analysis: A model selection perspective. *Multivariate Behavioral Research*, *48*(1), 28–56, https://doi.org/10.1080/00273171.2012.710386.

R Core Team (2018). R: A language and environment for statistical computing. Vienna, Austria: R Foundation for Statistical Computing. Retrieved from https://www.r-project.org/

Roberts, B., Harris, M. G., & Yates, T. A. (2005). The roles of inducer size and distance in the Ebbinghaus illusion (Titchener circles). *Perception*, *34*(7), 847–856, https://doi.org/10.1068/p5273.

Schoups, A. A., Vogels, R., & Orban, G. A. (1995). Human perceptual learning in identifying the oblique orientation: Retinotopy, orientation specificity and monocularity. *The Journal of Physiology*, *483*(3), 797–810, https://doi.org/10.1113/jphysiol.1995.sp020623.

Schwarzkopf, D. S., & Rees, G. (2013). Subjective size perception depends on central visual cortical magnification in human V1. *PLoS One*, *8*(3): e60550, https://doi.org/10.1371/journal.pone.0060550.

Schwarzkopf, D. S., Song, C., & Rees, G. (2011). The surface area of human V1 predicts the subjective experience of object size. *Nature Neuroscience*, *14*(1), 28–30, https://doi.org/10.1038/nn.2706.

Shaqiri, A., Pilz, K. S., Cretenoud, A. F., Neumann, K., Clarke, A., Kunchulia, M., & Herzog, M. H. (2019). No evidence for a common factor underlying visual abilities in healthy older people. *Developmental Psychology*, *55*(8), 1775–1787, https://doi.org/10.1037/dev0000740.

Shrout, P. E., & Fleiss, J. L. (1979). Intraclass correlations: Uses in assessing rater reliability. *Psychological Bulletin*, *86*(2), 420–428.

Simpson, W. A., & McFadden, S. M. (2005). Spatial frequency channels derived from individual differences. *Vision Research*, *45*(21), 2723–2727, https://doi.org/10.1016/j.visres.2005.01.015.

Spang, K., Grimsen, C., Herzog, M. H., & Fahle, M. (2010). Orientation specificity of learning vernier discriminations. *Vision Research*, *50*(4), 479–485, https://doi.org/10.1016/j.visres.2009.12.008.

Spearman, C. (1904a). "General Intelligence" objectively determined and measured. *The American Journal of Psychology*, *15*(2), 201–292.

Spearman, C. (1904b). The proof and measurement of association between two things. *The American Journal of Psychology*, *15*(1), 72–101, https://doi.org/10.1037/h0065390.

Thurstone, L. L. (1944). *A factorial study of perception*. Chicago, IL: The University of Chicago Press.

Tulver, K. (2019). The factorial structure of individual differences in visual perception. *Consciousness and Cognition*, *73*, 167–177, https://doi.org/10.1016/j.concog.2019.102762.

Tulver, K., Aru, J., Rutiku, R., & Bachmann, T. (2019). Individual differences in the effects of priors on perception: A multi-paradigm approach. *Cognition*, *187*(3), 167–177, https://doi.org/10.1016/j.cognition.2019.03.008.

Verhallen, R. J., Bosten, J. M., Goodbourn, P. T., Lawrance-owen, A. J., Bargary, G., & Mollon, J. D. (2017). General and specific factors in the processing of faces. *Vision Research*, *141*, 217–227, https://doi.org/10.1016/j.visres.2016.12.014.

Wang, L. L. (2010). Disattenuation of correlations due to fallible measurement. *Newborn and Infant Nursing Reviews*, *10*(1), 60–65, https://doi.org/10.1053/j.nainr.2009.12.013.

Ward, J., Rothen, N., Chang, A., & Kanai, R. (2017). The structure of inter-individual differences in visual ability: Evidence from the general population and synaesthesia. *Vision Research*, *141*, 293–302, https://doi.org/10.1016/j.visres.2016.06.009.

Webster, M. A., & MacLeod, D. I. A. (1988). Factors underlying individual differences in the color matches of normal observers. *Journal of the Optical Society of America A*, *5*(10), 1722–1735, https://doi.org/10.1364/JOSAA.5.001722.

Wechsler, D. (2003). *Wechsler Intelligence Scale for Children–Fourth Edition (WISC-IV)*. San Antonio, TX: The Psychological Corporation.

Wexler, M. (2005). Anticipating the three-dimensional consequences of eye movements. *Proceedings of the National Academy of Sciences, USA*, *102*(4), 1246–1251.